NUMBER 113 FEBRUARY 2008

AAO NEWSLETTER

ANGLO-AUSTRALIAN OBSERVATORY

Pathfinder for an International Large Optical Telescope

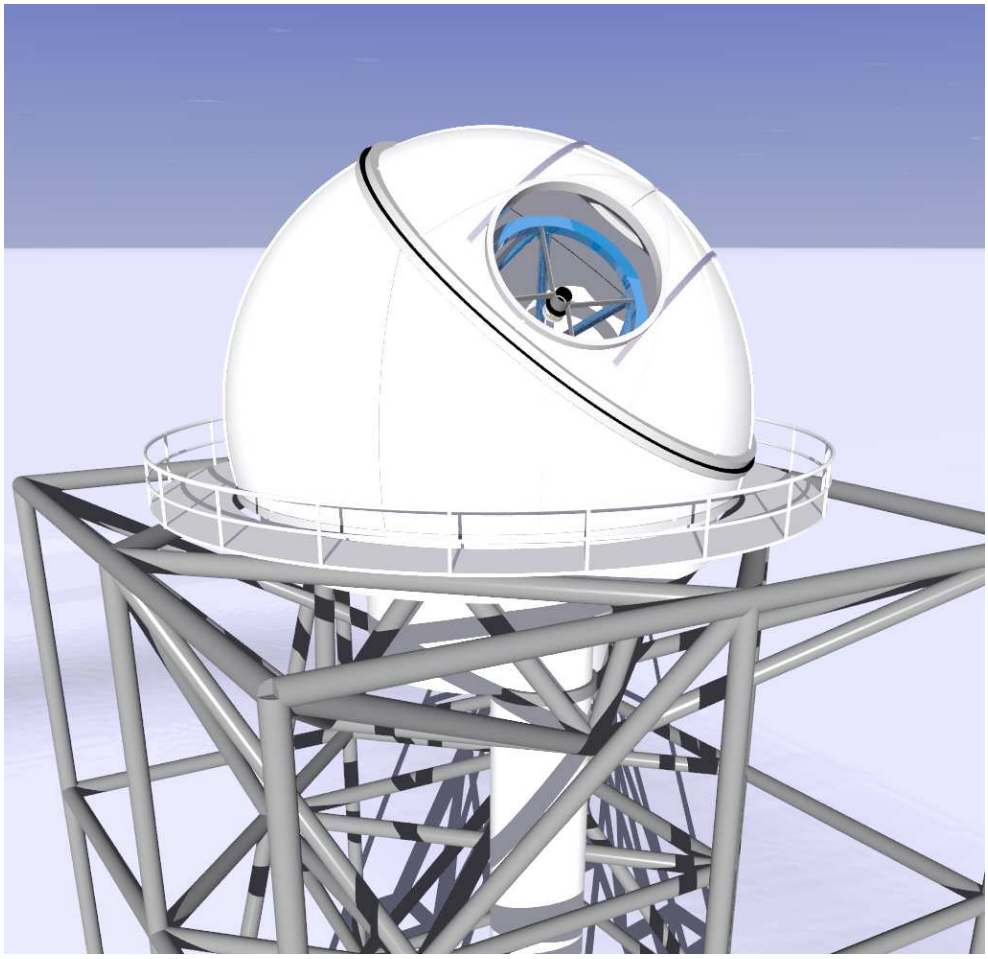

An artist's impression of the Pathfinder for an International Large Optical Telescope (PILOT) which is proposed for Dome C on the Antarctic Plateau. In this issue of the newsletter the members of the PILOT team provide a broad review of the design and capabilities of this proposed facility. In addition, Will Saunders of the AAO outlines the potential of PILOT for exploring the equation of state of the Universe through high-precision weak lensing observations..

contents

4 Searching far and near in the UKIRT Infrared Deep Sky Survey (Kuenley Chiu et al.)
8 Star forming galaxies at $z \sim 0.24$ (Eduard Westra & Heath Jones)
13 Design and capabilities of PILOT (Will Saunders et al.)
17 PILOT: a strong case for weak lensing (Will Saunders)
21 New instrument for the AAT – High Resolution Multi-Object Echelle Spectrograph (Sam Barden)
23 AAT new instrument workshop – Summary, conclusions & actions (Matthew Colless)
26 Improved precision of 2dF fibre positioning (Russell Cannon et al.)
32 Astronomy and ritual warfare in ancient Peru (Fred Watson)

DIRECTOR'S MESSAGE

This edition of the Newsletter has a focus on some of the projects at the AAO that are being funded under the Australian government's National Collaborative Research Infrastructure Strategy (NCRIS). These include the PILOT design study for an Antarctic telescope, a new instrument for the AAT, and the relocation of the Australian Gemini Office to the AAO.

The front cover of this Newsletter shows a visualization of a design for the PILOT telescope that is being proposed for Dome C on the Antarctic Plateau. The design of this 2.4-metre telescope has a number of unique features that allow it to not just survive in Antarctic conditions but also to exploit the extraordinary atmospheric qualities that potentially make the Antarctic Plateau the best optical/infrared site on the planet. Together with the University of New South Wales (UNSW), the AAO is funded through NCRIS to carry out a design study that will refine the science case for PILOT and present a costed concept for the telescope and its instrumentation. An outline of the design and capabilities of PILOT is given in the article by Will Saunders et al. on page 13 of this Newsletter. A second article by Saunders on page 17 argues that PILOT's high spatial resolution over a wide field makes it an extremely powerful facility for large-scale weak lensing studies. The PILOT design study is due for completion by the middle of this year, and will provide a secure foundation on which to build Australia's plans for Antarctic astronomy.

Another NCRIS-funded project underway at the AAO is a new instrument for the AAT. In November last year the AAO held a workshop to bring together and compare the various concepts that have been under consideration for the AAT. I summarise the discussions and conclusions of that meeting in the article on page 23. The bottom line is that the AAO is proposing to proceed with HERMES (pronounced as Hermes), a High-Resolution Multi-object Echelle Spectrograph. HERMES can be viewed as a high-resolution arm for AAOmega – like AAOmega, it uses the existing 2dF top-end optics and fibre positioning robot, so that it can observe about 400 objects simultaneously. However, while AAOmega operates at low to medium spectral resolution (R~1,000–10,000) and can cover the full optical range in a single observation, HERMES will operate at R~30,000 and cover about 400Å in one observation. Further preliminary technical specifications are given in the article by Sam Barden on page 21. The primary science driver for HERMES is Galactic archaeology: untangling the complex formation history of the Galaxy by mapping the phase-space orbits and chemical abundances of its component stellar associations. However HERMES is a highly versatile instrument with some unique capabilities, and it will have applications across broad swathes of astronomy. In particular, HERMES will extend the survey approach that the AAT is renowned for in extragalactic astronomy and cosmology to important questions in Galactic and stellar astronomy.

The third NCRIS-funded program highlighted here is the relocation of the Australian Gemini Office (AusGO) to the AAO. Up until now the AusGO has been a movable feast, following the location of the Australian Gemini Scientist of the time to different institutions around the country. Now, with new funding arrangements for Australia's participation in Gemini, the AusGO has been given a permanent home at the AAO. The new Australian Gemini Scientist is Stuart Ryder, and he outlines the role and functions of the AusGO in an article on page 37. Later this year he will be joined by Terry Bridges, as one of two Deputy Gemini Scientists, the other of whom will be located at Mount Stromlo. Expect to see more articles on Gemini-related topics in future editions of this Newsletter!

The fundamental mission of the AAO is to provide optical and infrared observing facilities that enable its user community to do outstanding science. This mission can be broken down into three essential activities: first, to provide high-quality access to the best existing facilities – as we aim to do for Gemini through the AusGO; second, to provide uniquely capable instrumentation for those facilities – such as we are building in HERMES; and, third, to develop world-leading facilities for the next generation – such as PILOT. These projects, together with the AAO's other on-going programs, form a coherent and balanced plan for the Observatory's future.

Matthew Colless

LARGE OBSERVING PROGRAMS ON THE AAT FOR SEMESTER 08B

The AAO aims to provide opportunities for Australian and British astronomers to make effective use of the Anglo-Australian Telescope's unique capabilities to address major scientific questions through large observing programs. These large observing programs may use any instrument, or combination of instruments, on the AAT, although the community's particular attention is drawn to the AAOmega spectrograph, which will be the world's most efficient instrument for large-scale survey spectroscopy for some years to come.

In line with previous announcements, the AAT Board (AATB) is issuing this *Request for Proposals (RfP)* for major new observing programs to commence in semester 08B (August 2008 to January 2009) or semester 09A (February 2009 to July 2009. Note, however, that programs extending beyond semester 10A may possibly be subject to modification following the end of the current AAT Agreement in June 2010. The AATB expects large observing programs to be awarded more than 25% of the available time on the AAT in semester 08B; this fraction of time will be reviewed for subsequent semesters. The AATB encourages ambitious large programs and does not set an upper limit on the fraction of time large programs can be awarded. All proposals will be evaluated by the Anglo-Australian Time Allocation Committee (AATAC), and should use the standard AATAC form (although with non-standard page limits). The case for the proposed large observing program must include:

1. A major, compelling and feasible scientific program. The proposal should focus on key questions that the observational data would address, but should also outline anticipated secondary uses of the data by the broader community. 'Major' in this context will generally mean programs requiring 50 nights or more (there is no set upper limit), possibly extending over several semesters. The science will be expected to be groundbreaking and not just incremental. Proposers need to discuss what their program will achieve in comparison with other on-going and future programs on similar timescales. *The scientific program should be described in no more than 5 pages (including figures, tables, and references).*

2. An observing strategy describing the provision of the input target sample, the detailed plan for the observations (number of nights including the standard allowance for weather, cadence of time-critical observations, and total duration of the project), the proposed instrumental setups, constraints on weather conditions or timing of observations, signal-to-noise or other figures of merit required to achieve the science goals, and any special support needed. The number of targets, required data quality, sensitivity limits and other relevant information should be rigorously justified. Programs requiring multiple visits to the same field should present a strategy for updating targets for optimum efficiency. *The observing strategy should be described in no more than 2 pages.*

3. A management plan outlining the collaboration involved in the program, the sharing of responsibilities for scientific management; the planning and carrying out of observations; data reduction; quality control at each of these stages; data release to the AAO community and the International Virtual Observatory; and finally, data analysis and exploitation by the team. The plan should outline the roles of all team members and how members contribute to carrying out the program. Proposers may also wish to suggest a publication strategy, including the process for determining authorship. *The management plan should be described in no more than 2 pages.*

4. A project timeline including the observations and analysis, with milestones and regular reviews by AATAC during the program. Proposers should plan for significant public outreach, and the proposal should explain the broader impact of the project. *The timeline and outreach should be described in no more than 1 page.*

Proposers are encouraged to form broad collaborations across the Australian and British communities in support of their programs; other international collaborators are welcomed. Proposers should also familiarise themselves with the revised procedures for time allocation that will apply from Semester 08B onwards (http://www.aao.gov.au/AAO/astro/newformula.html). The PIs for large programs will generally be expected to commit to the project as the main focus of their research over the program's duration.

Proposals for large observing programs should be submitted to AATAC by the standard proposal deadline of 15 March 2008.

Anyone considering submitting a large program proposal should contact the AAO Director (director@aao.gov.au) in advance to discuss their plans.

Matthew Colless
AAO Director

SEARCHING FAR AND NEAR IN THE UKIRT INFRARED DEEP SKY SURVEY

Kuenley Chiu (University of Exeter),
Andrew Bunker (AAO), and collaborators

When the Sloan Digital Sky Survey (SDSS) completed its baseline program approximately two years ago, the tally of its discoveries of objects such as the nearest brown dwarfs and the most distant high redshift quasars was unprecedented. While every survey seeks to extend our access to a new combination of wavelength coverage, areal coverage, and depth, the SDSS had provided a remarkable multitude and range of stellar, galaxy, and quasar science followup opportunities. Over the years new SDSS sources have been greatly exploited by telescopes from the smallest to the largest 8-metre observatories, by both ground- and space-based observatories, including the AAT and innovative instruments such as 2dF (most notably the 2SLAQ program, for example).

The followup of faint red objects was specifically encouraged by the SDSS inclusion of the *z′* filter, in combination with red-sensitive CCDs, allowing some of the first deep wide-field imaging beyond 8500Å. By selecting objects present in the *z′* filter, and appearing in no other bands blueward of these wavelengths (called the *i*-dropout technique), we and many collaborators found new examples of previously speculated classes of objects – particularly late brown dwarfs (T class), which due to their very low stellar temperatures have their peak flux in the near-infrared, and high-redshift quasars (*z*~6), which only begin to have strongly visible flux in the *z′* band and beyond due to the absorption of the intervening intergalactic medium (IGM). The discovery of these populations, in part thanks to IRIS2 and 2dF on the AAT, illuminated significant new physical properties of these objects as well as their environments, for example by characterising the coldest stars yet known, and measuring the evolution of the diffuse IGM near the cosmological epoch of reionization. This fortuitous coincidence of flux in the longest optical

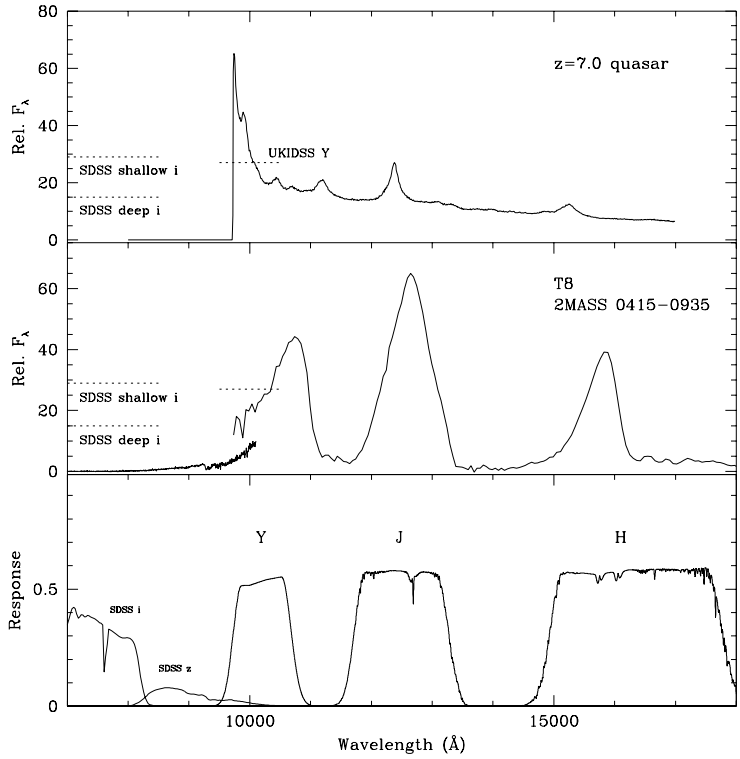

Figure 1: Quasars at *z*>6.4 and late T dwarfs (and Y dwarfs) display nearly no flux in optical bands (SDSS *i*/*z*), but strong flux in *Y*. This dropout (*i*-*Y*) provides the main target selection criterion in our program. However, imaging artifacts and objects such as uninteresting M stars are often also detected in UKIDSS *Y*, and fall just below the SDSS shallow detection limit. Their invariable selection requires us to carefully prescreen and reject objects using imaging such as with IRIS2. We also use deep SDSS optical imaging to obtain greater depth (lower dotted line, "deep"), eliminating many poor candidates and identifying genuinely large colour decrements. Model quasar at *z*=7.0 is from simulation work in Chiu et al. 2005, and T dwarf spectrum is constructed from optical/near-IR spectra of 2MASS 0415-0935.

wavelengths has allowed us interestingly, in one search, to find some of the nearest and most distant objects in the universe at the same time.

With the completion of the SDSS main survey, two new projects are seeking to continue the record of such discovery, with goals (among others) of pushing these samples to even more dramatic red and faint populations. The projects that may make this possible are the ongoing UKIDSS (UKIRT Infrared Deep Sky Survey) and the soon-to-be-commissioned VISTA (Visible and Infrared Survey Telescope for Astronomy). These two missions, which are 4-metre class wide-field imaging surveys with wavelength coverage beginning in the *Y* filter (1μm) and extending out to *K* band, represent a 3rd generation of near-IR surveys that promise a better match to the rapidly increasing optical data available compared with the legacy of 2MASS, for example. It is hoped that by pushing to fainter magnitudes and farther to redder near-IR wavelengths, even colder brown dwarfs beyond the T class and higher redshift quasars within the epoch of reionization will be discovered.

The Search

To date, we have been exploring the steadily increasing amount of UKIDSS imaging data (roughly 250 square degrees per semester) to identify and spectroscopically confirm high redshift quasars and brown dwarfs further into the red. WFCAM (Wide-Field Camera) on UKIRT is an impressive and fast instrument, reaching a depth of [*Y,J,H,K*]=[20.2, 19.6, 18.8, 18.2] (5σ, Vega) in the 40 second nominal survey exposure time, and covering a tiled area of 0.78 square degrees in a standard 2x2 mosaic pattern. This provides a good match to optical data, especially the SDSS, which reaches [*ugriz*]=[22.0, 22.2, 22.2, 21.3, 20.5] (5σ, AB). The UKIDSS Large Area Survey (LAS), which overlaps strategically with the SDSS footprint, is the region of interest for our search, and we employ the matched catalogs of these two datasets to find red objects. But while relatively straightforward in theory, a few observational considerations make the procedure interesting, and we describe the process briefly here.

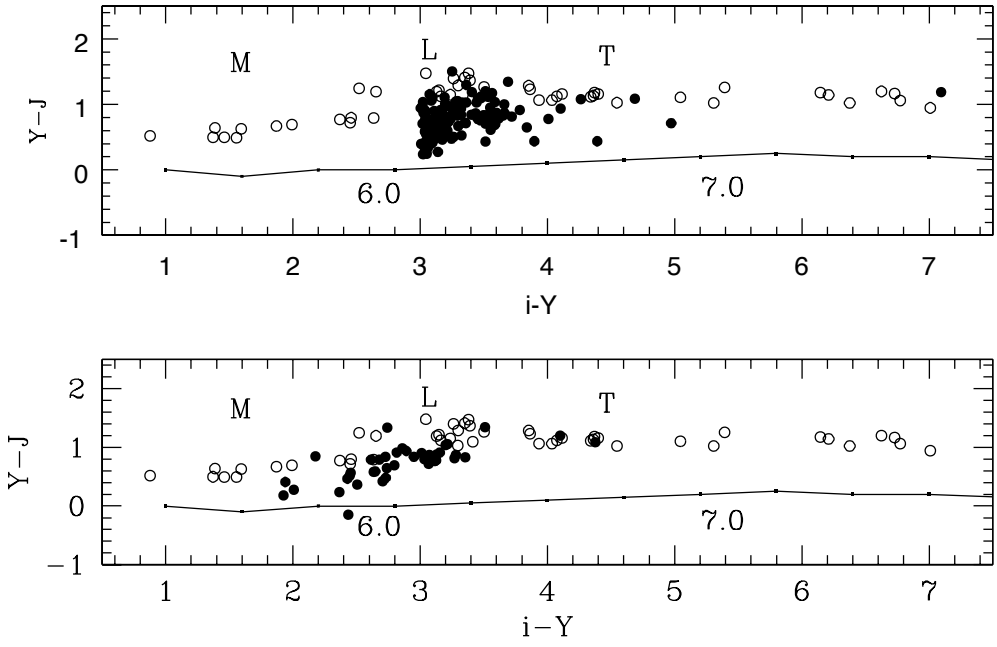

Figure 2 : These two panels show how deeper optical data can greatly assist with the identification of true quasar and brown dwarf candidates. The top panel shows the candidates (solid black points) as extracted from the database (after visual inspection), and that significant numbers of similar catalog objects in a given area would have to be observed down to a colour decrement of interest (*i-Y*>3.0) using normal methods. In the bottom panel, merging with deep SDSS optical data immediately reveals the true colour decrement of many candidates, and allows only the most promising genuine objects to be efficiently selected for followup. An order of magnitude less followup effort is required to reach the same faintness/colour limit. Dwarf stellar locus: open circles with MLT labels, and quasar locus: solid line with numeric redshift labels.

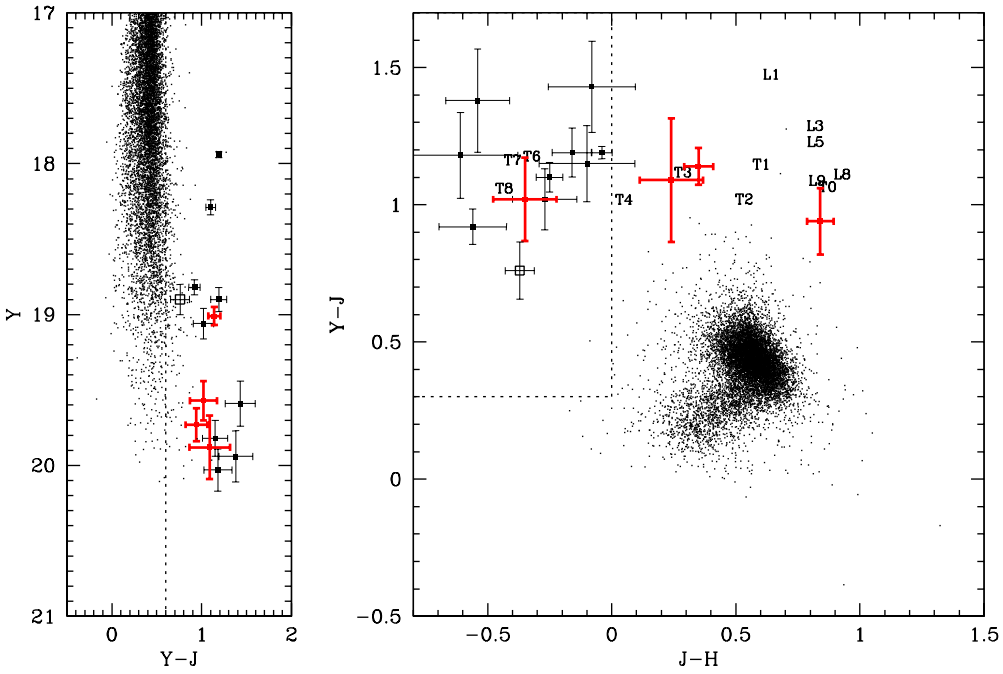

Figure 3: The four faint T dwarfs we discovered are plotted (red points with thick error bars) in (*Y-J*) versus *Y* colour-magnitude (left) and *YJH* colour-colour (right) diagrams. Normal stars are shown as small points, and the concurrently discovered objects of Lodieu et al. are shown for comparison (black points with light error bars). The extremely late-type T8.5 dwarf of Warren et al. is the open square with error bars. In the left panel, the dotted line indicates the typical *Y-J*>0.6 selection cut used to identify dwarf candidates. In the right panel, the dotted rectangular region indicates the range of predicted colours for late T and Y dwarfs. Small text labels follow the approximate locus of brown dwarf example types.

When seeking brown dwarfs and quasars, we generally identify sources from the imaging catalogs that are bright in UKIDSS Y or J, and faint (or undetected) in SDSS *i* or *z* bands. These objects (with large *i-Y*, for example, see Fig. 1) should be the coldest brown dwarfs and high-redshift quasars due to their rising SEDs towards the near-infrared. However, in practice, large numbers of contaminants can emerge from the databases along with the genuine candidates – e.g. imaging artifacts, moved objects, and normal stars of low colour decrement at the detection limit. Because of the single epoch and shallow depth of SDSS and UKIDSS, when selecting for the most interesting sources the reliability of candidates can be severely reduced even by a small percentage of contaminants present in the larger sample. These contaminants masquerade as good candidates in colour space, sometimes causing followup observations to be spent on false or uninteresting targets.

Eliminating contaminating sources thus represents a large fraction of the effort expended in the preparation and initial identification of candidates, and where possible, we have used special deep imaging to greatly reduce this problem. Multiple epoch coverage of areas such as the SDSS Southern Equatorial Stripe, reaching >1.25 magnitudes deeper than the normal SDSS coverage, has allowed image coadding (and rejection) of many types of contaminants, greatly reducing the time spent on inspection of objects and more quickly revealing promising candidates for followup. Then, our basic technique is to seek objects with large i-band dropouts (*i-Y*> ~3, see Figure 2), and UKIDSS sources completely undetected in the SDSS.

Following this initial selection, our candidates typically number less than ~0.5 per square degree, and are subjected to followup imaging. This is undertaken to confirm the reality of sources, measure the faint *i/z* flux of the objects, and to confirm the near-IR photometry of the new WFCAM images. These followup images are taken at 4-metre class telescopes, and in the past we have used IRIS2 at the AAT in addition to similar near-IR imagers at SOAR (Cerro Pachon), UKIRT, and APO, for example. Typical exposure times in the near-IR and optical are fairly brief – usually less than 300 seconds is needed to confirm and obtain photometry for the depths of our typical sample.

Following imaging verification, those objects with still interesting colours are observed spectroscopically. Optical spectroscopy at 7000Å and beyond is used to

identify the possibility of any emission lines (indicating a quasar), and if no emission is found (indicating a likely brown dwarf), further spectroscopy in the near-infrared is carried out, such as with IRIS2, the SpeX instrument (IRTF), or in faint cases, GNIRS (Gemini). From a comparison of the near-IR spectrum with reference templates, the spectral type of any brown dwarf object can be derived.

Current Status

So far, the search by our group and others has definitely been more successful at finding brown dwarfs than high-*z* quasars (with dwarf discoveries beating quasars by approximately 10:1), for a number of reasons. First, the physical number density of average T dwarfs selected by this technique at any magnitude range greatly outnumbers the density of quasars, and thus naturally more dwarfs are discovered (as was also the case with SDSS). Many hundreds of square degrees may need to be searched to find the next (or first) truly extreme-redshift quasar. Secondly, dwarfs are more amenable to being found in the data because their spectral characteristics cause flux to be generally strongly detected in two or more bands if it is detected at all (note the strong *J* and *H* band flux in addition to *Y* flux in the dwarf spectrum). Quasars, on the other hand, have a very blue spectral index, and may drop out of the longer wavelength bands if *Y* flux is already only marginal or weakly detected. Thus, quasar selections are more susceptible to contaminants, i.e. they require more numerous followup attempts to sort out genuine candidates.

Nevertheless, since late 2006, we have searched through the UKIDSS data releases using this procedure, and have independently found 4 T dwarfs (as well as several more in collaboration with the UKIDSS cool dwarfs working group, CDSWG). These dwarfs range down to some of the coldest and latest types known (see Figure 3), and the sample has been followed up with additional observations to understand the interesting physical aspects of the population, such as laser guide star observations to probe binarity. We used the IRIS2 instrument extensively to obtain these results, and it was most productive in the imaging/screening and deeper photometric characterization portions of the search, especially given the flexibility to change targets and plans dynamically according to our observations even on the same night. We have used our findings from the Southern Equatorial Stripe (the special SDSS region spanning 22^h to 4^h along +/–1.25° dec), to compare the expected numbers of brown dwarfs predicted from theoretical star formation models, which may help to guide future search plans.

Finally, two relatively high redshift quasars have been found by others using the UKIDSS data (one at z=5.86 by Venemans et al., and one at z=6.11 by Mortlock et al.), indicating that there may be good potential for discovery of a quasar at z>6.4 given the gradually increasing imaging area with each semester. It is interesting to note, however, that both of these objects appear in, and could have been selected from, SDSS data alone (although addition of the near-IR undoubtedly made the discoveries more likely). Therefore, the question of whether the most dramatic possible discovery – a z>6.4 quasar which relies on a complete non-detection in SDSS – will eventually be made with UKIDSS data, remains open. And we will be continuing to look for the answer.

References

Four Faint T Dwarfs from the UKIDSS Southern Stripe. Chiu, K., et al. 2007, arXiv0712.1229. in press, MNRAS

Eight New T4.5-T7.5 Dwarfs Discovered in the UKIDSS LAS DR1. Lodieu, N., et al. 2007, MNRAS, 379, 1423

The Optical and Near-IR Properties of 2837 Quasars in the UKIDSS. Chiu, K., Richards, G.T., Hewett, P.C., Maddox, N. 2007, MNRAS, 375, 1180

The Discovery of the First Luminous z~6 Quasar in the UKIDSS LAS. Venemans, B.P., et al. 2007, MNRAS, 376, 76

STAR FORMING GALAXIES AT $z \sim 0.24$

Eduard Westra (RSAA) & Heath Jones (AAO)

It is widely accepted that the amount of star formation in the Universe as a whole has increased since the formation of the first galaxies, peaking around redshifts $z \sim 2$–3 and subsequently declining by a factor of 10 (e.g. Hopkins 2004, and references therein). This cosmic star formation history provides important constraints on e.g. galaxy formation and evolution (Pei et al. 1999; Somerville et al. 2001), because it directly traces the accumulation of stellar mass and metal fraction (Pei & Fall 1995; Madau et al. 1996) to their present-day values (Cole et al. 2001; Panter et al. 2003). Its rapid decline over the past 8 Gyr is consistent with 'downsizing' scenarios (Cowie et al. 1996) in which the more-massive galaxies have produced their stellar mass at earlier times than the less-massive galaxies (Heavens et al. 2004; Juneau et al. 2005; Thomas et al. 2005; Fardal et al. 2007). The star formation history of the Universe has also been used to constrain allowable stellar initial mass functions (Baldry & Glazebrook 2003; Hopkins & Beacom 2006) and cosmic supernova rates (Gal-Yam & Maoz 2004; Daigne et al. 2006).

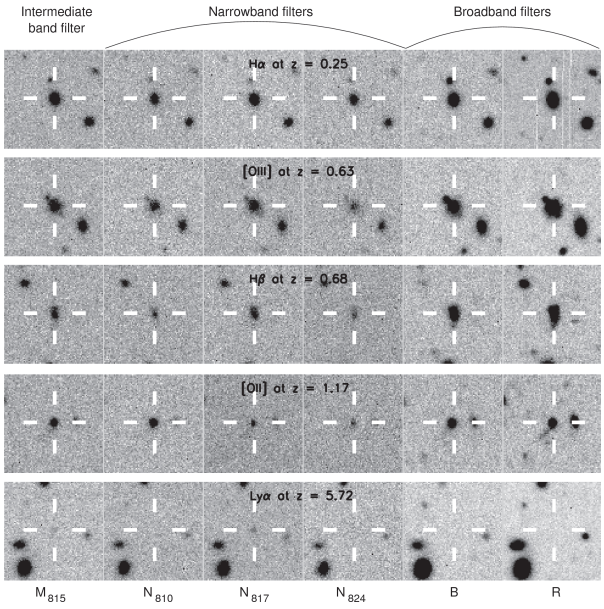

Figure 1: Postage stamp images (19" on a side) of emission line galaxies at different redshifts as seen through our narrowband survey. From left to right, frames show intermediate band (*FWHM* = 220 Å at 8150 Å), three narrowband (*FWHM* = 70 Å at 8100, 8170 and 8240 Å) and broadband *B* and *R* images. Observe how the galaxy is brightest in the N_{817} filter in all cases, except for the $z = 1.17$ galaxy, where it is N_{810}. The redshifts of these galaxies have been confirmed using spectroscopy.

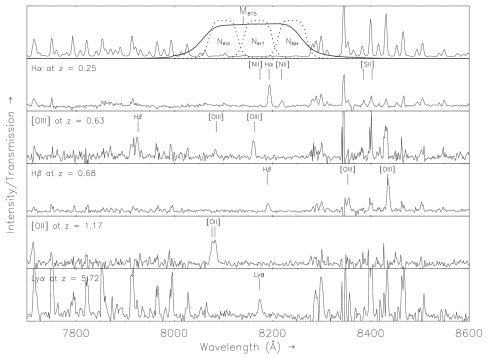

Figure 2: AAOmega spectra of the same emission line galaxies as shown in Figure 1. The top panel shows the night-sky spectrum alongside the intermediate and narrowband filter-profiles used for galaxy selection. Key emission lines are indicated. All spectra, including the Lyα emitter at $z = 5.72$, have been taken using the AAOmega spectrograph.

A variety of star formation indicators exist across the electromagnetic spectrum that either probe the UV flux of newborn stars directly or infer it through indirect means. At low redshifts, the most-direct calibrator – and of the optical calibrators the least affected by internal extinction – is the Hα recombination line. Here, we summarise the results of a survey for Hα emission line galaxies at $z \sim 0.24$ using AAOmega spectroscopy of galaxies selected from the Wide Field Imager Lyman Alpha Search (WFILAS; Westra et al. 2005, 2006) taken with the Wide Field Imager on the ESO/MPI 2.2m telescope at La Silla Observatory.

Emission lines are a typical feature in the spectra of star forming galaxies. The most distinctive ones in the optical are, from blue to red, [OII] $\lambda\lambda$3726,3728, Hβ λ4863, [OIII] $\lambda\lambda$4959,5007 and Hα λ6564. Narrowband surveys are a powerful tool to find these emission line galaxies at any redshift (e.g. Thompson et al. 1995). In Fig. 1 we show five emission line galaxies at widely different redshifts selected in the six different filters of our survey: an intermediate band filter, three narrowband filters and two broadband filters. In each case, the object is significantly brighter in the narrowband filter used to capture the emission line. In Fig. 2 the results of AAOmega spectroscopy for the same galaxies are shown. The spectral region covered by the intermediate and narrowband filters is also shown in Fig. 2.

Candidate selection

We used SExtractor (version 2.3.2; Bertin & Arnouts 1996) in double-image mode to create the initial source catalogues. Each resulting catalogue contains the photometry for the sources in

all six filters. The following four criteria were applied to select our candidate emission line galaxies from the initial source catalogues:

(i) The narrowband image used as the detection image must have the most flux of all the narrowband images and the source must have a 4σ detection or better in the detected narrowband.

(ii) There must be at least a 2σ detection or better in the intermediate band image.

(iii) The broadband image *R* needs to have a 2σ detection or better.

(iv) The emission line flux calculated from the narrowband images should be $F_{line} \geq 10^{-16}$ erg s^{-1} cm^{-2} after aperture corrections.

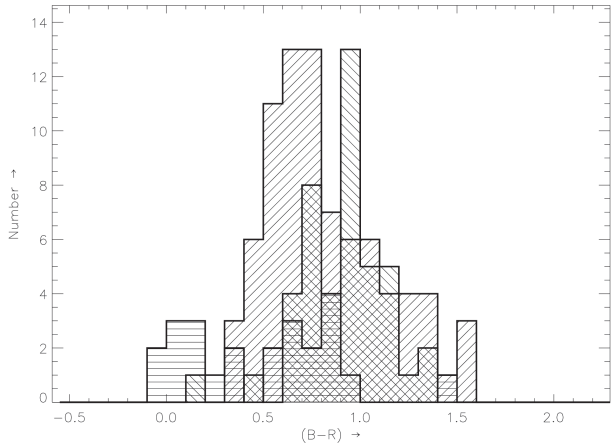

Figure 3: Observed (*B*-*R*) colour distribution for various sets of emission line galaxies within our sample: (a) Hα at $z \sim 0.24$ (*forward cross-hatching*), (b) [SII] at $z \sim 0.21$ (*backward cross-hatching*) and (c) single-line emitters of indeterminate origin (*horizontal cross-hatching*).

Stars represent a significant fraction of contaminants. We found that standard star/galaxy classification from SExtractor works satisfactorily for objects brighter than $R = 21$. However, it breaks down for the large number of faint ($R > 21$) objects. Therefore, additional criteria were applied. We examined the size of the objects (major- and minor-axis), in combination with their shape (the ratio of the major- and minor-axis) as additional star/galaxy discriminants. We used an additional cut in (*B*-*R*) colour [$(B\text{-}R) \geq 1.4$ to prevent the unwanted removal of unresolved line emitting galaxies] based on the unrestricted (*B*-*R*) colour distribution of $z \sim 0.24$ Hα emitters and $z \sim 0.21$ [SII] emitters. Finally, we removed objects that showed obvious imaging artefacts, such as diffraction spikes or ghost images, in any of its thumbnails.

From initial candidate numbers of 786 and 848 for the two fields, 414 and 513 candidates were removed because they met one or more of the stellar criteria. Our final sample yielded 372 candidate emission line galaxies for the CDFS field and 335 for the S11 field.

AAOmega spectroscopy

The above selection criteria are sensitive to almost any galaxy with emission lines that have been redshifted into the wavelength range of our narrowband filters and are bright enough to be detected. The one exception is Lyα, which does not yield detectable flux bluewards of the Lyman limit and hence in our broadband images. Since our goal was to establish the star formation density at $z \sim 0.24$ we concentrated only on those galaxies detected as Hα.

We used AAOmega spectroscopy to determine which emission line fell in our narrowband filters. Other groups (e.g. Ly et al. 2007) have separated objects based on their broadband colours. However, as our data show, the colours of [SII] galaxies ($z \sim 0.21$) are indistinguishable from those with Hα ($z \sim 0.24$) due to their similar redshifts. When local large-scale structure conspires to populate the foreground at $z \sim 0.21$, selection strategies that rely on colour alone are not sufficient. Figure 3 shows how the Hα and [SII] galaxies occupy the same range of colour [$(B\text{-}R) > 0.5$], given their near-identical redshift. Based on this distribution, we classify all the single-line emitters, which could not be identified due to the lack of accompanying lines, outside this range as likely [OII] emitters at $z \sim 1.2$. It is worth pointing out that when the [SII] doublet falls inside our narrowband filter set, an extra volume of about 50% of the volume probed by Hα can be explored. Unfortunately, the fluxes of [SII] and Hα are not sufficiently correlated to permit star formation density determinations from the [SII] line (e.g. Kewley et al. 2001).

For fields with a high density of targets, such as our fields, only ~250 of the 392 fibres could be allocated per configuration, due to the placement limitations of the fibre buttons. In general, the number of fibres allocated depends on the target distribution in the field and the choice of algorithm in the configure software. We found that using the Simulated Annealing algorithm (Miszalski et al. 2006) allowed a larger fraction of fibres to be allocated to candidates than did the older Oxford algorithm.

The AAOmega data were taken during four separate runs. The first observations were done in classical mode during two nights, 2006 March 23 and 24. During this run only one of our fields was observed. The other three occasions were done in service mode on 2006

October 10, 2006 November 10 and 2007 March 26. During these runs both fields were targeted. We used the 580V and the 385R VPH gratings for the blue and red arm, respectively. In total, 301 and 255 candidates were observed in the two fields.

Basic spectral reductions, including bias-subtraction, flat-fielding and wavelength-calibration, were done using the DRCONTROL software[1]. The final one-dimensional spectrum for each object was obtained by averaging the reduced spectra of the object in the different observations using our own IDL scripts. Finally, we observed several standard stars taken during the final night of the 2006 March run to determine the system throughput as a function of wavelength and the sensitivity curve of each standard star. These curves were scaled to a common level and averaged to give the overall sensitivity. This was applied to all the science spectra to flux-calibrate each relative to one another.

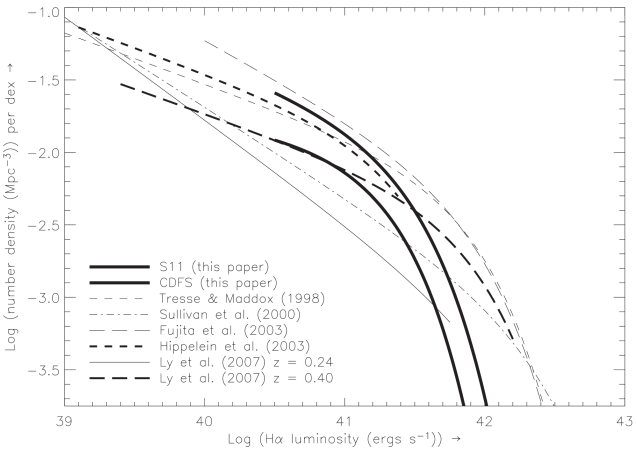

Figure 5: Comparison of the Schechter functions derived for our two fields (thick solid lines) and those of other surveys. The Schechter function of each survey has been drawn over the luminosity range where data were available.

Luminosity function and star formation density of Hα emitting galaxies at $z \sim 0.24$

With the final emission-line catalogue in hand, our approach to calculating the Hα luminosity functions is as follows. We take our measured distribution of line emitters (all emission lines from all redshifts) from the narrowband candidate sample and apply the following:

(i) Corrections for incompleteness in the original narrowband imaging. This is less than 0.1% for all galaxies over the relatively bright line fluxes used.

(ii) Corrections for incompleteness in the spectroscopic observations. We used a Monte Carlo simulation to assess the spectroscopic completeness as a function of line flux. We modelled the emission lines in several high signal-to-noise spectra of Hα galaxies, subtracted the model and added a randomly scaled version of this model with a random offset in wavelength to the remaining noise. We then attempted to re-identify any emission line. This exercise demonstrated the potential to identify at least 90% of the galaxies at a line flux of $F_{line} = 10^{-16}$ erg s^{-1} cm^{-2}.

(iii) The spectroscopically measured fraction of Hα emitters as a function of flux. Of the candidates for which we have spectroscopically confirmed an emission line (189 and 117 out of the total 301 and 255 observed in each field), just under half are Hα at $z \sim 0.24$, a quarter are [SII] at $z \sim 0.21$, roughly a sixth are Hβ or [OIII] at $z \sim 0.6$–0.7 and the remainder are [OII] at $z \sim 1.2$.

(iv) Extinction correction. We calculated the extinction for all Hα galaxies using the measured ratio of the Hα and Hβ lines in the stacked spectrum of our Hα galaxies (see Fig. 4) after correction for stellar absorption.

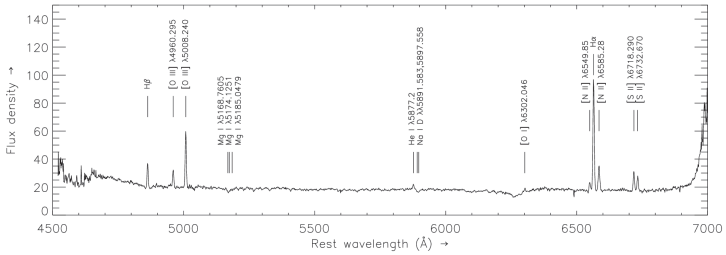

Figure 4: Mean red-arm spectrum of emission-line galaxies from the CDFS field. Spectra from 114 galaxies between $z \sim 0.19$ and 0.27 were de-redshifted before stacking. The most-prominent features have been labelled. The apparent absorption feature just bluewards of the [OI] λ6302 line is the remnant of the telluric *A* band of the individual spectra being de-redshifted and stacked.

1 DRCONTROL is a software package produced and maintained by the AAO. It can be obtained from ftp://ftp.aao.gov.au/pub/2df.

This gives us a value for $A_{H\alpha}$ = 0.96 assuming a Cardelli et al. (1989) extinction law.

After the application of the corrections we fit a Schechter function for which the Schechter parameters are (α, log L^*, log φ^*) = (–1.33 ± 0.34, 41.43 ± 0.22, –2.23 ± 0.32) for one field and (–1.11 ± 0.51, 41.24 ± 0.25, –2.28 ± 0.33) for the other.

In Fig. 5 we compare our Schechter fits to the results of other surveys using Hα as a measure for star formation. We restricted the comparison to Hα surveys with z <~ 0.40 in order to limit the systematic uncertainties which play into the comparison when different star formation indicators are involved. It can be seen that there is a large range in each of the Schechter parameters between surveys. The wide span of parameters could be attributed to evolution of the luminosity function, as has been suggested by Hopkins (2004) and Ly et al. (2007), who compare surveys over a wider redshift range using different indicators. However, a number of systematic uncertainties exist between surveys that could also be attributed to the scatter between the luminosity functions. We now discuss each of these below.

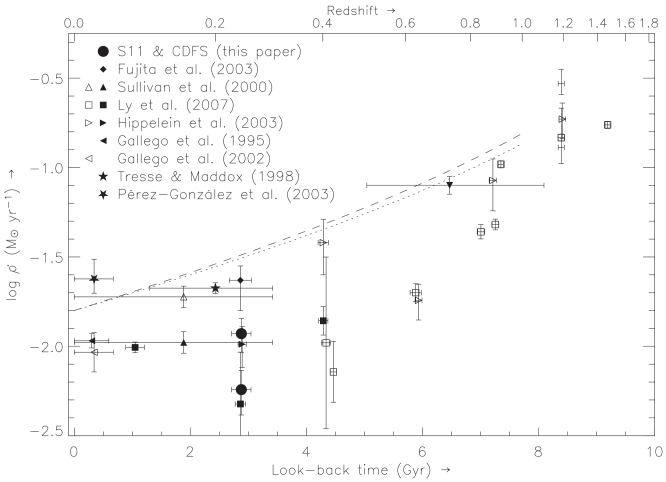

Figure 6: Star formation density as a function of look-back time derived from emission-line surveys, where the Schechter function has been integrated from the star formation rate corresponding to the flux limit of our survey, 1 x 10^{-16} erg s^{-1} cm^{-2} (0.33 M_{sun} yr^{-1}). The solid symbols represent the star formation density derived from the Hα line, the open symbols from either the [OII] or the [OIII] line. Our fields are indicated by the solid circles. The dotted and dashed lines are the least-squares fit from Figs. 1 and 2 of Hopkins (2004), respectively. They are not corrected for the fact that Hopkins (2004) integrated the Schechter function down to L = 0 erg s^{-1} and are indicated for comparison purposes only.

– The details of galaxy selection inevitably vary from survey to survey. Some surveys select galaxies using either a blue or red broadband filter. Passbands that favour bluer and/or star-forming galaxies generally yield higher faint-end counts and thus steeper slopes. This undoubtedly has a similar influence on the faint-end slope of the Hα luminosity function.

– Our survey uses a flux cut-off rather than an equivalent width cut-off (or likewise, a narrowband – broadband colour). An equivalent width cut-off will tend to be biased against galaxies with low equivalent widths. This will affect mostly the selection of galaxies with a high star formation rate (SFR) per unit continuum, such as early-type spirals and galaxies with low Hα flux in general.

– The amount of extinction is not well determined. Although our value agrees with that found by other surveys, there is still a large spread in extinction values. A range of $A_{H\alpha}$ = 0.5 – 1.8 is typical of those found. This range translates directly into an uncertainty of 0.3 in log L^*, unless the extinction for each individual galaxy has been measured.

– There is only a limited spectroscopic follow-up on candidate line-emitting galaxies in many surveys, or none at all. Spectroscopy on several sources in e.g. Ly et al. (2007) shows that slight contamination of higher redshift emission-line galaxies occurs in their Hα sample. As we noticed in our follow-up, there is a large sample of galaxies that have been selected on their [SII] lines in one of our two fields, which would have been mistaken for low-redshift Hα had we relied on colour selection alone. If we had not included the separation of [SII] and Hα galaxies in our analysis, the star formation density for this field would have been overestimated by ~30%.

– Spectroscopic observations also allow flux corrections for the [NIII] lines that straddle the Hα line. We have not included corrections for this, because the range of contribution to our Hα flux ranges from –7% up to +14% for the wide range of metallicities found in these galaxies.

– Cosmic variance has been widely cited as a major contributor to the differences between various surveys (e.g. Ly et al. 2007). We are well placed to test this, given our observations of two distinct fields that have been subjected to identical selection and analysis. We use the prescription of Somerville et al. (2004) to determine the relative cosmic variance for our survey. The corresponding cosmic variance over our survey volume translates to an uncertainty in log φ(L) of +0.2/–0.3, which is ample to account for the difference between the luminosity functions of the two fields.

Star formation density

We can derive global star formation densities from Hα luminosity densities, since the amount of extinction-corrected Hα luminosity from an HII region is directly proportional to the star formation rate. The luminosity density is obtained by integrating the Schechter function. This yields for luminosities $\geq L_{lim}$

$$\mathcal{L} = \varphi^* L^* \Gamma(\alpha + 2, L_{lim}/L^*)$$

In the case of some surveys, the faint-end slope of the Hα luminosity function is poorly constrained, thus having important consequences for the integrated luminosity density. To overcome these, we calculate the star formation density of other emission-line surveys at similar redshifts by assuming a common fixed star-formation limit rather than integrating from zero. We chose volume-average SFR = 0.33 M_{sun} yr^{-1}, which corresponds to the limit of our survey (L_{lim} = 10^{-16} erg s^{-1} cm^{-2}). This avoids faint-end extrapolations or lessens the influence of the faint-end fits assumed by those surveys. This yields volume-average SFR = –2.24 +0.11 –0.14 and –1.93 +0.08 –0.10 for our fields.

These results are indicated in Fig. 6 together with those of other surveys after they have been transformed to the same cosmology and limiting star formation rate. Observe that the star formation density in both our fields agrees well with other Hα emission-line surveys at the same redshift. Nevertheless, there is a difference of almost 1 dex between the highest and lowest values for the star formation density. We have also plotted the star formation density fits of Hopkins (2004) in Figure 6, which make use of values integrated down to zero luminosity, unlike the points. This serves to illustrate the extent to which extrapolation of the faint-end fit affects the final determination of star formation: typically up to <~ 50% for $\alpha \sim -1.3$ (larger for steeper values).

Obviously, the same systematic uncertainties for the luminosity functions as discussed above will also play a role here. Furthermore, we compared surveys over a larger redshift range, hence other emission-line star formation indicators have been used, thereby introducing their own sources of systematic uncertainty, such as larger extinction corrections and an abundance dependence for the star formation calibrator.

Summary and conclusions

We report the results of a survey for Hα-emitting galaxies at $z \sim 0.24$. We used two fields from WFILAS. It consists of imaging in three narrowband filters (*FWHM* = 70 Å) and an encompassing intermediate band filter (*FWHM* = 220 Å) supplemented with broadbands *B* and *R*. A total of 707 candidate emission-line galaxies were identified (after removal of stellar contaminants). Using spectroscopy from AAOmega, we identify the nature of the emission line and determine the fraction of emitters that is Hα at $z \sim 0.24$. We determine the Hα luminosity functions for both our fields after applying this fraction, imaging completeness, spectroscopic completeness and extinction corrections. There are some differences between the luminosity functions of the fields and between other surveys at similar redshifts, hence, also in the luminosity density, but these are dominated by cosmic variance and differences in selection criteria, respectively. We note that spectroscopic follow-up is essential to remove confusion between Hα-emitters at $z \sim 0.24$ and [SII]-emitters at $z \sim 0.21$.

Acknowledgements

We are indebted to Rob Sharp for his suggestions on preparing and reducing the AAOmega observations and for his help during the observations. We are also grateful to AAO service observers Will Saunders and Quentin Parker. EW acknowledges the AAO for its hospitality and financial support during visits to Epping.

References

Baldry I.K. & Glazebrook K., 2003, ApJ, 593, 258
Bertin E. & Arnouts S., 1996, A&AS, 117, 393
Cardelli J.A., et al., 1989, ApJ, 345, 245
Cole S., et al., 2001, MNRAS, 326, 255
Cowie L.L., et al., 1996, AJ, 112, 839
Daigne F. et al., 2006, ApJ, 647, 773
Fardal M.A., et al., 2007, MNRAS, 379, 985
Fujita S.S., et al., 2003, ApJ, 586, L115
Gallego J., et al., 1995, ApJ, 455, L1
Gallego J., et al., 2002, ApJ, 570, L1
Gal-Yam A. & Maoz D., 2004, MNRAS, 347, 942
Heavens A., et al., 2004., Nature, 428, 625
Hippelein H., et al., 2003, A&A, 402, 65
Hopkins A.M., 2004, ApJ, 615, 209
Hopkins A.M. & Beacom J.F., 2006, 651, 142
Juneau S., et al., 2005, ApJ, 619, L135
Kewley L., et al., 2001, ApJ, 556, 121
Ly C., et al., 2007, 657, 738
Madau P., et al.., 1996, MNRAS, 283, 1388
Miszalski, et al., 2006, MNRAS, 371, 1537
Panter B., et al., 2003, MNRAS, 343, 1145
Pei Y.C. & Fall S.M., 1994, ApJ, 454, 69
Pei Y.C., et al., 1999, ApJ, 522, 604
Pérez-González P.G., et al., 2003, ApJ, 591, 827
Somerville R.S., et al., 2001, MNRAS, 320, 504
Somerville R.S., et al., 2004, ApJ, 600, L171
Sullivan M., et al., 2000, MNRAS, 312, 442
Thomas D., et al., 2005, ApJ, 621, 673
Thompson D., et al., 1995, AJ, 110, 963
Tresse L. & Maddox S.J., 1998, ApJ, 495, 691
Tresse L., et al., 2002, MNRAS, 337, 369
Westra E., et al., 2005, A&A, 430, L21
Westra E., et al., 2006, A&A, 455, 61

DESIGN AND CAPABILITIES OF PILOT

Will Saunders, Peter Gillingham, Andrew J. McGrath, David Ward, Roger Haynes. (AAO), John Storey, Jon Lawrence, Michael Burton (UNSW)

Introduction

PILOT (Pathfinder for an International Large Optical Telescope) is a 2.4m optical/infrared telescope, proposed for Dome C on the Antarctic Plateau, with target first light at the end of 2012.

Conditions at Dome C are known to be exceptional for astronomy. The seeing (above ~30m height), coherence time and isoplanatic angle are all twice as good as at Mauna Kea, while the water vapour column, and sky and telescope thermal emission are all an order of magnitude better (Lawrence et al. 2004, Agabi et al. 2006 , Walden et al. 2005.).

PILOT is a key step to a major international observatory at Dome C. The specific aims of PILOT are to:

- demonstrate that large optical telescopes can be built and operated in Antarctica with reasonable timescale and cost;
- show that we can fully utilise the excellent natural seeing and thermal backgrounds at the site;
- characterise the possibilities for diffraction-limited observing from the site;
- perform cutting-edge science.

A design study by the AAO and UNSW, funded as part of Australia's National Collaborative Research Infrastructure Strategy (NCRIS), is currently underway, with completion planned for mid-2008. The primary aims of the design study are to produce a viable design and implementation plan, and a realistic costing. As part of the study, we are actively seeking partners in the PILOT project, and input into the design and the scientific requirements. This closely ties in to the FP6-funded ARENA network, to determine European priorities for Antarctic astronomy.

Further information on the PILOT project can be found at http://www.aao.gov.au/pilot/

Design overview

PILOT is a classic Ritchey-Chrétien telescope. The size is determined by commercially available designs, by the availability of ion-beam mirror polishing, by the limits for passive mirror support, and by the scale of atmospheric turbulence at Dome C.

PILOT will have twin Nasmyth foci, f/1.25 primary, and an overall speed of ~f/10, giving an image scale of 8.6"/mm. It will be installed on a 25–30m tower, above the turbulent surface layer. It will be in a thermally and humidity-controlled enclosure and will allow 24 hour remote operation with minimal human intervention.

For wide-field work, the image quality and pixel scale are matched to the median, fast tip-tilt-corrected, free seeing (see below). However, provision is made for sampling diffraction-limited images at all wavelengths longer than 500nm.

The optical design has evolved during the study. A Gregorian design was originally preferred, because of the conjugacy of the secondary with residual boundary layer turbulence. However, in practice the gain is small compared to large penalties in telescope length, cost and field of view. Narcissus mirrors were originally envisaged (Gillingham 2002), but the current design is much warmer than Gillingham assumed (because it is at 30m elevation), the field of view is larger and the intention now is to make PILOT a much more general-purpose telescope; these considerations lead us to a design with a cold stop within the infrared instruments.

Enclosure and tower

On the Antarctic Plateau, there is strong surface turbulence caused by the katabatic wind flowing off the plateau together with a strong vertical temperature gradient; the surface level seeing is no better than at Siding Spring. However, this layer is only tens of metres deep. Extensive site testing at Dome C indicates that a telescope at 30m elevation will be above most of this turbulence for most of the time, and that the median wintertime seeing at this height is ~0.3". For this reason, PILOT is proposed to be placed on a tower, of a design (Hammerschlag et al. 2006) that is extraordinarily stiff to twisting and bending. The expected residual windshake is <0.2" (Lanford et al. 2006). This will be reduced further, by factors of several, by the fast tip-tilt secondary.

It would be possible to mount the telescope at surface level, and use a Ground-Layer Adaptive Optical system to correct for the surface turbulence. However, this has major penalties in terms of field of view and wavelength coverage, as well as complexity. A GLAO system good enough to deliver diffraction-limited images at K_{dark} for a telescope at surface level would allow diffraction-limited images at 500nm for the same telescope on a tower. This seems to us a better use for such a system.

Two other major challenges at Dome C are the enor-

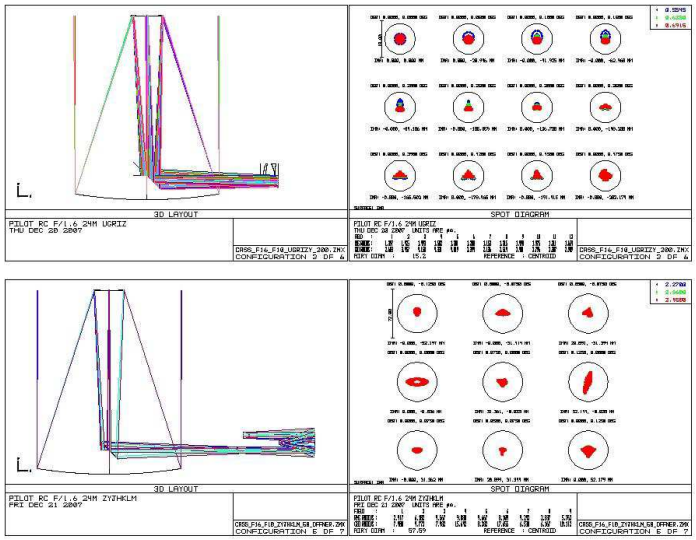

Figure 1: Optical layout and spot diagrams for PILOT in (a) wide-field optical use over a 1° (400mm) diameter field, with two silica corrector lenses; and (b) for wide-field NIR (1-5μm) use over a 15 arcmin (100mm) diameter field, with two CaF_2 corrector lenses and an Offner relay type cold stop. Spot diagrams are for *r* and K_{dark} band use. Airy discs are shown in both cases.

mous vertical temperature gradient, (~1°C/m at ground level and ~0.1°C/m even at 30m) and the supersaturated humidity (with respect to ice), despite being about the driest place on Earth! Both of these drive us towards a temperature and humidity-controlled dome, to avoid mirror seeing and frosting problems. The dome may be a calotte (as shown on the front cover), or a more traditional design.

Proposed instrumentation suite

A full suite for PILOT might comprise the following instruments:

Wide-field NIR (1–5μm) camera.

This would have at least 1, and possibly 4, 4K x 4K HAWAII-2RG arrays. The plate scale is 0.154"/pixel for 18μm pixels, allowing us to sample the diffraction-limit at K_{dark} and longer. Filters would be *zyJHK*$_{dark}$*LM*, with other filters still to be chosen, but probably including L_{dark} (2.9μm). To sample diffraction-limited imaging at *zyJH* bands requires a larger plate scale; this is achieved by introducing a Barlow lens doublet and fold mirrors into the optical path.

Very wide field optical camera

The accompanying article on page 17 shows that, with the use of PANSTARRS-type Orthogonal Transfer CCDs, we can achieve 0.2" FWHM image quality at *i*-band, with Strehl ratios ~0.25, across degree-sized fields. The proposed camera has a focal plane 400mm (1°) in diameter, with ~10μm pixels giving 0.086"/pixel sampling. If OTCCDs are not available, STA 10Kx10K detectors with 9μm pixels would be an excellent fall-back. Filters would be *ugriz*, with the remaining filter options still undecided. Detectors would be optimised for far red (*riz*) use, since it is here that the science gains are greatest.

High resolution, high speed optical camera for lucky imaging

Short exposure images will have a ~50% chance of being diffraction-limited at *i*-band in median conditions. So a camera based on an E2V L3-Vision detector (which allows fast readout without read noise) is an obvious first-light instrument, allowing cutting-edge science ('Hubble from the ground') straight away. It would be 1K x 1K, with ~0.025" pixels. This camera, with a simple Shack-Hartmann module, would also allow efficient guide star monitoring for a future upgrade to a full adaptive optical system.

Mid-infrared camera with Fabry-Perot filters

It is proposed that we have a 10–25μm camera, based on the Aquarius 1K x 1K detector, with ~2"/pixel, with narrow band filters allowing a survey of Galactic H_2 emission at 12 and 17μm. This survey would be possible during the daytime. An outline design has been provided by Mora et al. (2008).

Optical design

The mirrors will likely be lightweighted Zerodur or equivalent, since this offers excellent thermal stability, reasonable strength and low risk. All mirrors will be silver coated to minimise infrared emissivity. The need for active optical control of the primary is still under consideration. The secondary mirror will have a fast tip-tilt capability.

Each of the wide-field instruments will contain two corrector lenses, one of which will also form the dewar window. The optical raytracing gives diffraction-limited imaging longward of 0.5μm, across the entire field of view, for all the proposed instruments.

The target image quality delivered by the optics is 0.1" FWHM (or 80% encircled energy diameter 0.24").

Image quality

As well as correcting for windshake, the tip-tilt secondary gives significant adaptive optical improvement, especially in the NIR. We have modelled the C_N^2 profiles determined by Agabi et al. (2006), and we find that

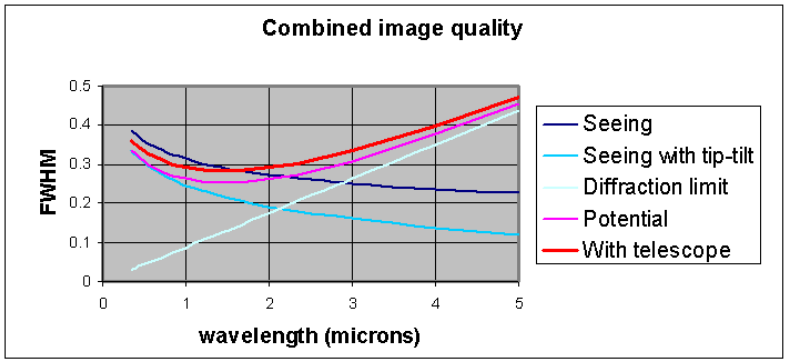

Figure 2: Anticipated image quality for PILOT, as a function of wavelength, and including contributions from tip-tilt-corrected seeing, diffraction, and telescope.

residual surface layer turbulence just above the telescope is largely cleaned up by this, across the entire field-of-view, and of course better at longer wavelengths. This partly compensates for the increasing diffraction limit at longer wavelengths, so the overall image quality is rather constant. For the expected median natural seeing of 0.3" FWHM at 500nm, the expected delivered image quality for 1–2.5μm varies in the range 0.28–0.3" (Figure 2).

In the far red (0.7–1μm), much better image quality, ~0.2", is in principle achievable over arbitrarily large fields, using tip-tilt correction for high-level turbulence (see accompanying article by Saunders).

Thermal backgrounds

The sky backgrounds are shown in Figure 3. To this must be added thermal background from the telescope. The typical winter temperature (at 30m elevation) is about –46°C, or around 50°C colder than for a temperate site, so the telescope emission is lower by an order of magnitude or more. However, the *relative* importance of sky and telescope emission is much the same at Dome C as at other sites, so cold stopping is just as important. We have produced a design with an Offner-relay-type reflective cold stop, but transmissive designs are also possible (Mora et al. 2008). The target emissivity for PILOT (3 mirrors + spider) is <5%.

Sensitivity

The tip-tilt corrected seeing, optical quality and backgrounds calculated above give the point source sensitivities listed in Table 1.

Science drivers

The science potential for PILOT has been extensively discussed in Burton et al. (2005), and is also currently

Table 1

Band	λ	Δλ	Sky (Jy)	Sky (AB)	1hr, 5σ (AB)
V	0.55	0.09	6E-6	22.0	27.3
R	0.69	0.15	1E-5	21.4	27.3
I	0.8	0.15	2E-5	20.7	26.8
z	0.9	0.15	8E-5	19.2	26.1
Y	1.0	0.2	2E-4	18.2	25.6
J	1.2	0.26	5E-4	17.2	25.2
H	1.65	0.29	1E-3	16.4	24.8
Kdark	2.4	0.23	1E-4	18.9	25.6
Ldark	2.9	0.2	2E-3	15.7	23.7
L	3.8	0.65	2E-1	10.7	21.5
M	4.7	0.24	5E-1	9.7	20.2

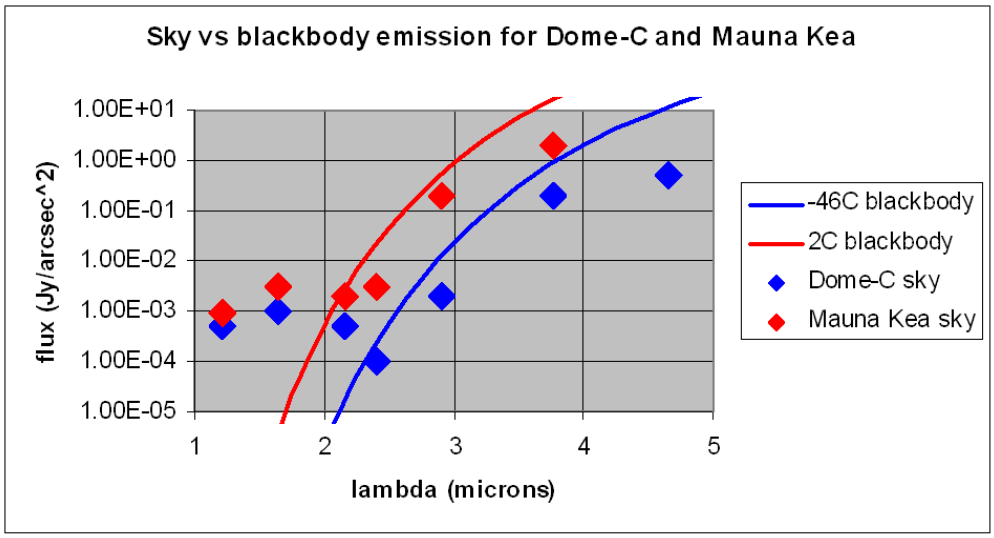

Figure 3: Relative thermal emission from a blackbody and from the sky, for Dome C (assumed –46°C) and Mauna Kea (2°C). The target emissivity for PILOT is <5%.

under study by the European ARENA network. The science case continues to evolve, and the current design focuses on four main science drivers:

A wide-field, high resolution, deep K_{dark} survey

The sensitivity gain over temperate sites is largest in the K-band, because the sky background is 20–30 times darker. PILOT cannot compete for depth with JWST, but JWST's areal coverage is limited (just as with HST) by the settling time and competition for telescope time as well as its field of view. Over large fields PILOT will be 2 magnitudes more sensitive than VISTA, or 2.5 – 10 times faster to cover an area to given depth (depending on the number of HAWAII-2 detectors). This means the data taken is of comparable depth to the deep optical surveys to be performed by VST and the Dark Energy Survey on the CTIO 4m.

Since this is the reddest band for which deep, wide-field data will be available, it is almost certain to lead to the highest redshift rare objects found by dropouts or unusual colours.

***L,M*-band followup of gamma-ray bursters**

The highest redshift gamma-ray bursters should reveal themselves through their *L, M*-band afterglow. Because the sensitivities at *L, M*-bands are so much better for PILOT than other terrestrial sites, and because space missions and larger telescopes cannot act in fast response, PILOT has by far the best prospects for any telescope to catch these afterglows, and obtain images and lightcurves for the most distant objects in the Universe.

A survey of Galactic H_2

H_2 in our Galaxy that is cooler than a few hundred Kelvin (i.e., all of it apart from the shock-heated material) is hard to map directly. The most important transition lines are in the mid-infrared, where sensitivities from the ground are very low. From space, the spatial resolution is very poor because of the small apertures. It is proposed to use PILOT during daytime at Dome C to map the Galactic H_2 through the 0–0 S(1) and S(2) transitions at 17 and 12μm. These lines are optically thin, and we would be able to map gas down to a temperature ~100K, allowing us to map the turbulently-heated gas.

Weak Lensing

The strong case for a weak lensing survey with PILOT is discussed in the next article in this edition of the newsletter.

References

Agabi, A., Aristidi, E., Azouit, M., Fossat, E., Martin, F., Sadibekova, T., Vernin, J. & Ziad, A. 2006, PASP, 118, 344

Burton, M.G., Lawrence, J.S., Ashley, M.C.B., et al. 2005, PASA, 22, 199

Hammerschlag, R.H., Bettonvil, F.C.M. & Jaegers, A.P.L. 2006, Proc. SPIE, 6273, 62731O

Lanford, E., Swain, M., Meyers, C., Muramatsu, T., Nielson, G., Olson, V., Ronsse, S., Vinding, N., Nyden, E., Hammerschlag, R. & Little, P. 2006, SPIE 6268E, 36

Lawrence, J. S., Ashley, M. C. B., Travouillon, T. & Tokovinin, A. 2004, Nat, 431, 278

Gillingham, P.R. 2002, PASA, 19, 301

Mora, A., Eiroa1, C., Barrado y Navascués, D., Persi, P. & Abia, C. 2008, 2nd ARENA conference, Potsdam

Walden, V.P, Town, M.S., Halter, B. & Storey, J.W.V. 2005, PASP, 117, 300

PILOT: A STRONG CASE FOR WEAK LENSING

Will Saunders, AAO

Introduction

Weak lensing has been widely identified as the most promising route to measuring the evolution of the equation of state of the Universe, and hence to understanding the nature of dark energy. A large number of huge lensing surveys are planned: PANSTARRS, LSST, The Dark Energy Survey on the CTIO 4m, KIDS on VST, HyperSuprimeCam for Subaru; and the DUNE and SNAP satellites.

For weak lensing, resolution is paramount, because the galaxies used to measure the effect are <1" in size, and must be at least partially resolved. Antarctica offers unique possibilities for wide-field, high-resolution imaging, so even modest sized telescopes may offer world-beating performance. This article is a preliminary investigation into the possibilities for measuring weak lensing with PILOT.

We assume a 2.4m f/10 telescope, with a 0.75deg^2 CCD camera, with image scale ~ 0.1"/pixel.

The size of lensed galaxies and effect of resolution on sensitivity

Figure 1 shows the size of galaxies detected in the Hubble Deep Field, as a function of AB magnitude. For AB=25–27^m, most galaxies are between 0.2" and 0.4", with only a weak dependence on magnitude. This means temperate-site observations, with image quality 0.6" or more, struggle to determine ellipticities for these galaxies. This is graphically shown in Figure 2, which compares space and (superb) ground-based images of the same field. All except the largest galaxies are dramatically circularised by the seeing.

The integration time required to measure ellipticity is a dramatic function of image quality, because (a) the intrinsic ellipticity of the galaxy is diluted by the PSF, and it must be observed to higher S/N to compensate, and (b) the observations are sky-limited, and the overall sky noise increases with the observed image size.

Suppose we are trying to measure the ellipticity of a galaxy of intrinsic FWHM $a \times b$, with observed dimensions (including seeing, telescope optics, pixellation) $A \times B$. Assuming Gaussian statistics, the time required to measure the ellipticity of a galaxy to a given S/N scales as

$$t_{req} \propto A\,B\,(A^2+B^2)(A+B)^2 / (a^2-b^2)$$

For a given intrinsic galaxy shape and size, t_{req} then varies as the *sixth power* of the observed image size. Figure 3 shows this effect of image size and seeing on the required integration time for fixed aperture, object brightness and background level. Galaxies smaller than the seeing are very difficult to measure because the apparent ellipticity is so small; large galaxies are difficult because the sky noise is large. The optimal size for target galaxies is 1–3 times the seeing, which means Dome C is ideally suited for this work. For typical galaxies, the required integration times at Dome C are one

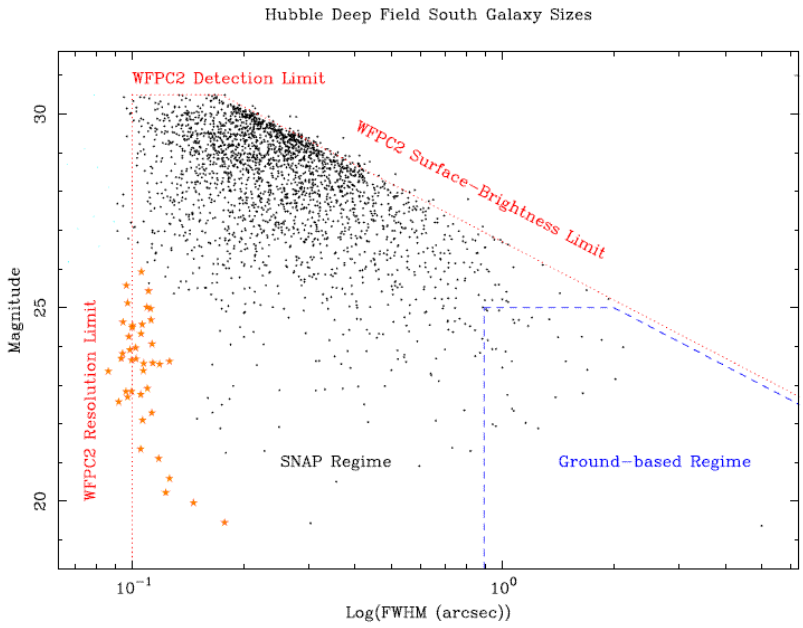

Figure 1. Image size for galaxies from the HDF, as a function of AB magnitude. Taken from Curtis et al. 2000.

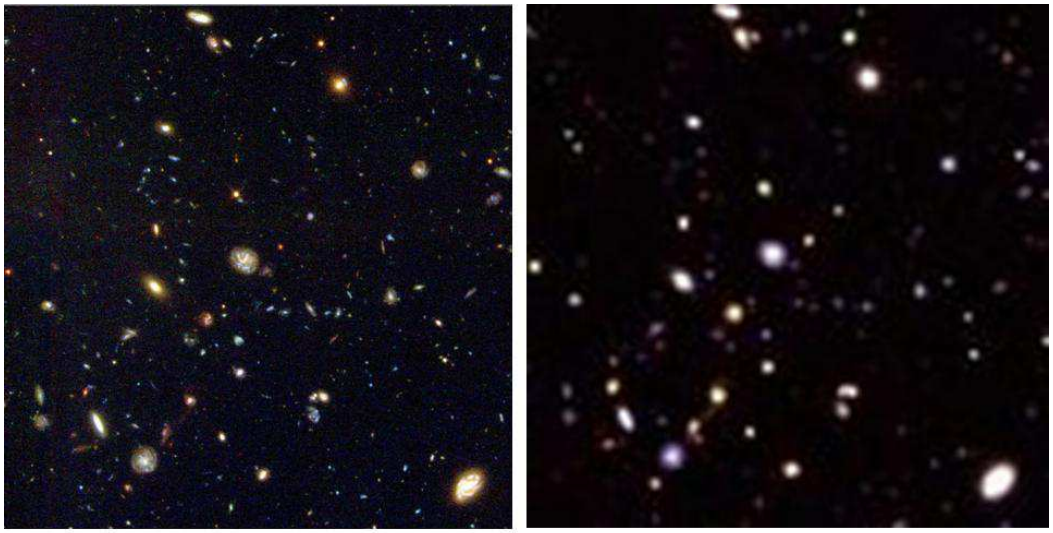

Figure 2. Effect of resolution on deep imaging. (Left) 0.1" FWHM (from HST) and (right) 0.5" FWHM (from VLT).

to two orders of magnitude less than for a similar telescope at Mauna Kea.

Of course, if we match the pixel scale to the median seeing, then worse seeing means we can image more sky at once for given detector area. Figure 4 shows the overall lensing survey speed as a function of image quality and galaxy size, for a telescope of fixed aperture and detector size, but with pixel scale matched to the seeing. The gain in overall survey speed between Dome C and the best temperate sites is still an order of magnitude.

Image quality with PILOT

The estimated PILOT wide field image quality, including median seeing, has been presented in the accompanying article. For *i*-band, the value is 0.3". This includes the effect of a fast tip-tilt secondary, which corrects for residual low-level turbulence above the telescope.

If we could correct for high level turbulence, we could improve the image quality much further. The median Fried length r_0 for PILOT at *i*-band is about 65cm, so $D/r_0 \sim 4$. This is exactly the regime where tip-tilt correc-

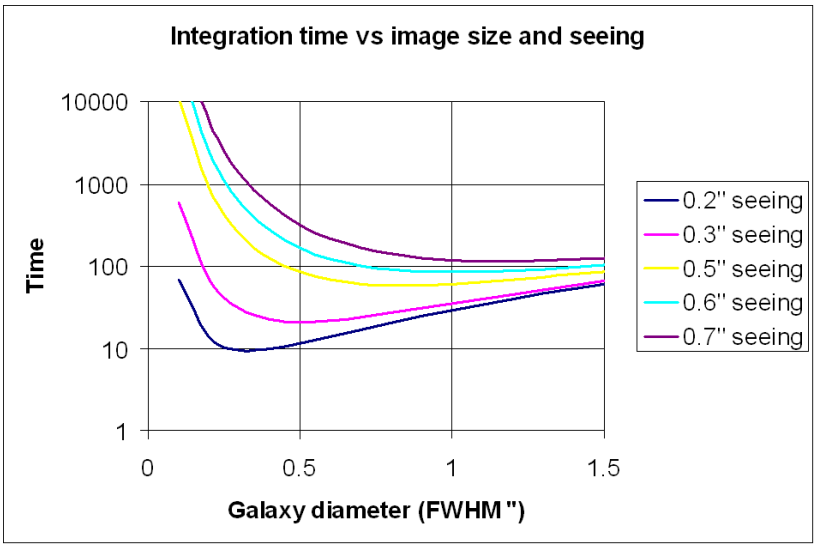

Figure 3. Required integration time per galaxy as a function of seeing and galaxy size.

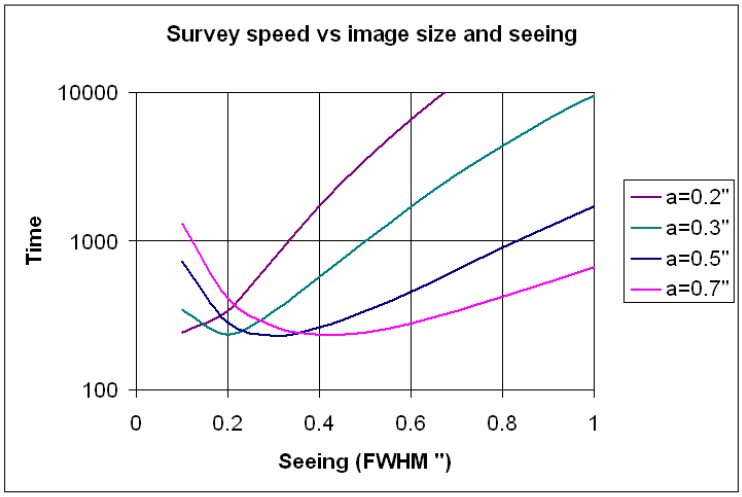

Figure 4. The overall survey speed as a function of seeing and galaxy size.

tion provides the largest gains (Hardy 1998, Jenkins 2000, Kaiser, Tonry and Luppino 2000, henceforth KTL). The angle over which the high level turbulence is correlated is much smaller than the field, so we have two requirements: a density of guide stars high enough to sample this turbulence, and some way of making differential tip-tilt corrections across the field. The latter could be achieved via a deformable mirror, but it could also make use of Orthogonal Transfer CCDs (Tonry, Burke and Schecter 1997), which allow charge shuffling in both directions, in ~500 × 500 pixel sub-arrays.

The required guide star density has been thoroughly investigated by KTL. They conclude that at Mauna Kea, the density of suitable guide stars is too low to map the required tip-tilt corrections over wide fields for a single telescope. However, at Dome C we have three large gains over Mauna Kea: (a) we can have a 2.5 times larger collecting area while preserving D/r_0 =4, (b) the Greenwood timescale is 3 times longer, and (c) the isoplanatic angle is 2.5 times larger (Agabi et al. 2006, Lawrence et al. 2004). So we can use fainter guide stars, and we can also tolerate larger separations between them. In overall terms of (guide stars)/(isoplanatic angle)^2, we are 20 times better off than Mauna Kea. This is enough to completely map the deflection field even at high latitudes, leaving negligible residual isoplanatic error (Figure 5).

The tip-tilt correction gives a 1/3 improvement in the encircled energy diameter. It also gives a significant diffraction-limited core containing 28% of the energy, with a Strehl ratio of ~0.25 (KTL, Jenkins 1998).

So we can expect diffraction-limited cores, with FWHM 0.07'', across the whole field. The limiting factor in practice will be the pixel size (0.075 – 0.1"), and the limited ability of OTCCDs to do sub-pixel shuffling. The gain in encircled energy can be fully utilised, to give us a FWHM ~ 0.2". This is perfectly matched both to our target galaxies, and to the pixel scale for the telescope (which is determined also by NIR considerations). It is better than the proposed DUNE satellite (0.23").

Comparison with other projects

For surveying ellipticities of typical faint galaxies, PILOT is at least an order of magnitude more efficient than a telescope of the same collecting and detector area at a

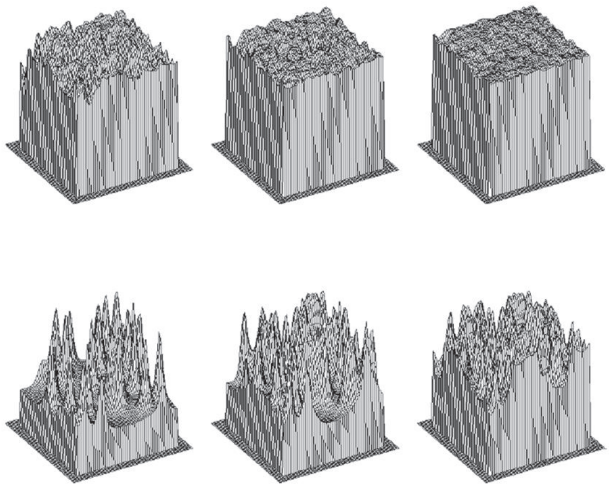

Figure 5. Strehl ratio achieved over a 1°×1° field as a function of the number of guide stars used to map the deflection field, for (from bottom left) 20, 40, 80, 160, 320, 640 guide stars. PILOT would have ~400 useable guide stars. The vertical axis runs from 0 to 0.25. Taken from Kaiser, Tonry and Luppino 2000, and scaled to Dome C atmospheric conditions.

temperate site. In practice, this means that we can reach surface densities not realistic elsewhere. It's very hard to reach densities higher than 10–20 galaxies/arcmin^2 even with 8m class telescopes, compared with 50–100 from space (e.g. Kasliwal et al. 2007). For PILOT, we should reach S/N = 10 for i_{AB}=26^m, 0.3" × 0.2" FWHM galaxies in 5000–10,000s, giving us ~50 galaxies/arcmin^2. A high space density is crucial for measuring the peak of the lensing power spectrum at l ~ 5000–10,000 (2–4'scales), which is where the greatest sensitivity to cosmological model occurs (Figure 6a). The higher resolution also means that the median depth of the lensed galaxies is greater than ground-based data, which increases (a) the sensitivity to lensing, (b) the volume surveyed, and (c) the lever-arm to measuring the evolution of the power spectrum.

Because the effects of lensing are so subtle, a fundamental limitation with ground-based imaging surveys is the constancy of the PSF across the field, and with time, elevation, colour, etc. PILOT has two large advantages over temperate telescopes: (a) the lensing signal is less diluted by resolution, so the sensitivity to systematic error is less by a factor of several, and (b) the PILOT optics deliver superb imaging, because of the slow f-ratio (f/10) and relatively modest field-of-view (1°), and because we have a Ritchey-Chrétien design. The optical design is diffraction-limited at *i*-band across the entire field.

There is also excellent overlap with the Dark Energy Survey, which will obtain photometry in *griz* bands, potentially giving photometric redshifts for the entire survey, and also the South Pole Telescope, allowing independent and robust determination of cluster masses, as a separate probe of the evolution of the power spectrum.

Compared with the DUNE satellite, a PILOT lensing survey looks remarkably good. The overall survey speeds, taking into account the image quality, sky background, aperture and field of view, are about the same. PILOT can only access ~ 1/4 of the high latitude sky. PILOT will not be capable of getting the deep *Y*, *J*, *H*-band data proposed for DUNE, but will be capable of obtaining deep *g*,*r* and also K_{dark} data if suitable data is not available elsewhere.

If 50% of dark and grey time is allocated to a lensing survey, PILOT could survey all accessible high latitude sky (about 5000deg^2) to i_{AB}=25^m in 4 years. On the (untested) assumption that adequate photometric redshifts can be obtained, then the overall signal-to-noise for cosmological parameter estimation is similar to that anticipated for DUNE (Figure 6b), but the survey would be completed by the time DUNE is launched.

References

Agabi, A., Aristidi, E., Azouit, M., Fossat, E., Martin, F., Sadibekova, T., Vernin, J. & Ziad, A. 2006, PASP, 118, 344

Curtis et al., 2000, SNAP proposal to DoE and NSF

Hardy,J.W. 1998. Adaptive Optics for Astronomical Telescopes, Oxford University Press, ISBN 0-19-509019-5

Jenkins, C.R. 1998, MNRAS 294, 69

Kasliwal,M.M., Massey,R., Ellis,R.S., Miyazaki,S., Rhodes,J. 2007, Astro-ph 0710.3588v1

Kaiser,N., Tonry,J.L., Luppino,G.A. 2000, PASP, 112, 768

Lawrence, J. S., Ashley, M. C. B., Travouillon, T. & Tokovinin, A. 2004, Nat, 431, 278

Tonry,J.L., Burke,B.E. and Schecter, P.L. 1997, PASP, 109, 1154

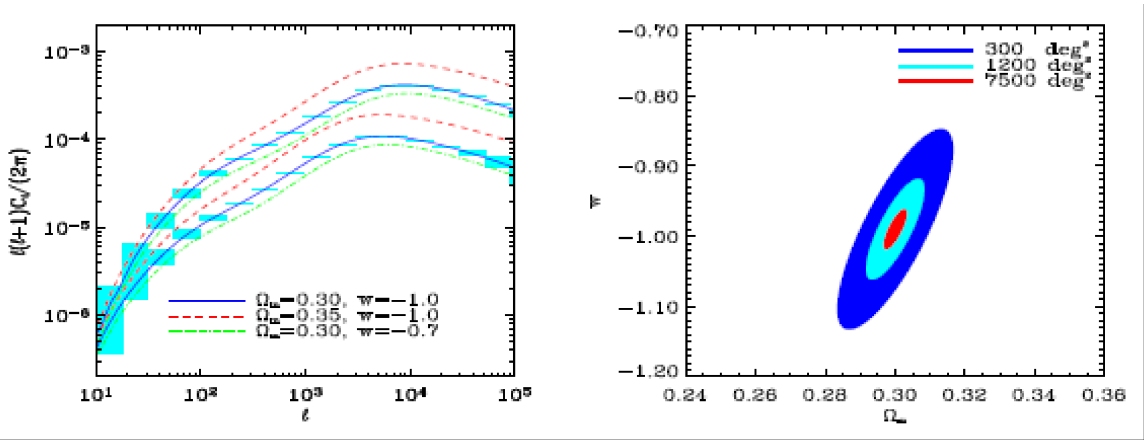

Figure 6a. Power spectrum and error bars for a weak lensing survey, of the depth proposed for PILOT, over 1200 deg^2. Figure 6b: Cosmological constraints for surveys of 300, 1200, 7500 deg^2. The proposed survey is for 5000 deg^2. Taken from the proposal to the ESA Cosmic Vision program.

NEW INSTRUMENT FOR THE AAT – HIGH RESOLUTION MULTI-OBJECT ECHELLE SPECTROGRAPH

S.C. Barden (Head of Instrumentation)

The instrumentation group is furthering the design development for the preferred instrument selected at the November community workshop (see the article on page 23 on the outcome of the community workshop). The instrument selected was the High Resolution Multi-Object Echelle Spectrograph (HERMES). Engineering effort is now focused on finalisation of a concept design to be ready for review this coming April.

The table below shows the initial set of science requirements to be achieved with HERMES for a major Galactic Archaeology survey and the compliance of the concept under study. Further science requirement definition is underway under the leadership of Ken Freeman at RSAA.

The current concept makes use of the existing AAOmega spectrograph by replacing the collimator with a "white pupil" capability and an echelle grating. The spectrograph will be reconfigurable to retain the classic AAOmega performance and capability, using just the pupil relay portion of the collimator (i.e. by avoiding the triple pass illumination of the collimator).

In high resolution mode (R=30k) the fibre slit is aimed so that the echelle grating is illuminated by the collimator. Since the detector real estate in the existing AAOmega cameras is insufficient to provide spectral coverage of nearly 400 Angstroms, two additional cameras are installed.

Consideration is also being given to an ultra-high resolution mode in which the echelle is swapped with a higher dispersion echelle to achieve spectral resolving powers of 50,000 to 60,000. Exploration of a cross-disperser for this mode is also under study. In this mode only

Item	*Requirement*	*Goal*	*Comment*	*Design Compliance*
Number of Objects	~400 per spectrograph	540 per spectrograph	Simultaneous targets per exposure	Yes
Spectral Resolving Power	30,000 nominal	40,000 nominal	$\lambda/\Delta\lambda$ FWHM	Meets requirement
Simultaneous λ Coverage	400 Å		Preferably in two comparable swaths (e.g. with dual channel camera) at 5500 and 6300 Å	Dual channel met, **but coverage is less than half required. This can be resolved with additional channels.**
Operable λ Range	390-950 nm	Same	Non-simultaneous	Yes
Main Wavelength Regime for optimal performance	550-650 nm	Same		Yes
Sensitivity	SNR =100 in 60 minutes at V=14		SNR is per resolution element	**TBD Peak efficiency should be ~10%**

10% of the fibres (40 fibres) are used. The goal is to achieve nearly 2000 Angstrom of spectral coverage.

The AAO will enable a public access web site where further information can be obtained and where you can follow the ongoing progress of this project.

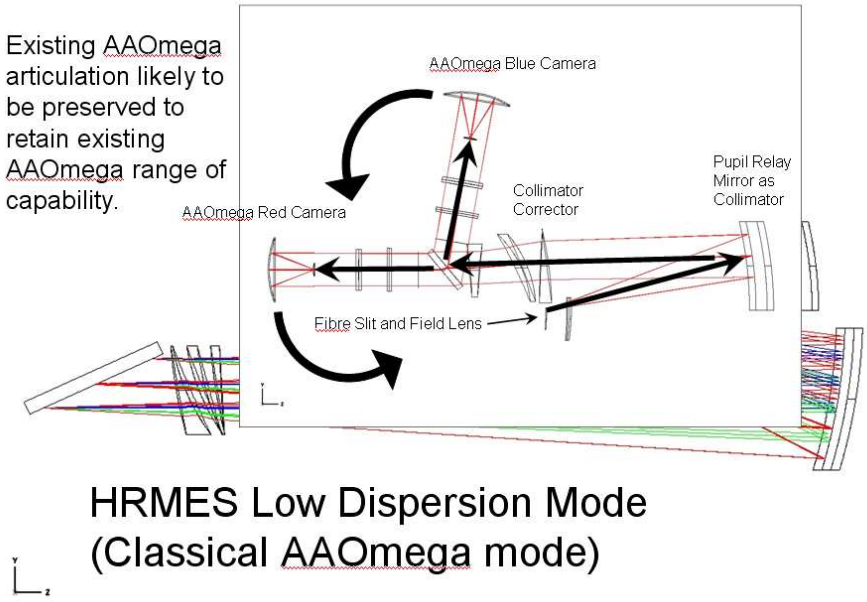

Figure 1 showing the classical AAOmega mode for HERMES.

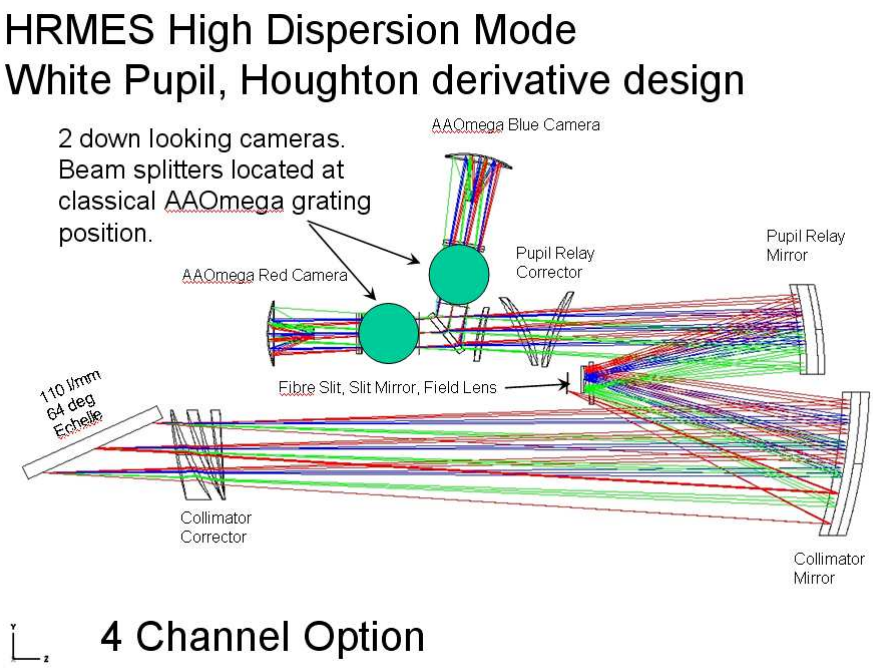

Figure 2 showing the R=30,000 mode for HERMES.

AAT NEW INSTRUMENT WORKSHOP – SUMMARY, CONCLUSIONS & ACTIONS

Matthew Colless

A lively and constructive community workshop was held at Epping on 9 November 2007 to discuss the options for the next major AAT instrument. The program and presentations can be found on the AAO web pages at http://www.aao.gov.au/conf/aatcommunity. The workshop drew 43 participants and produced a consensus on a number of important issues while raising some fresh ideas for further investigation.

Four main instrument concepts were discussed: AAOmicron, HERMES, WFMOS-A and NG1dF. This article reports the pros and cons for each instrument that emerged during the workshop, together with some of the issues and concerns raised during the discussion session. It finishes with a summary of the main conclusions from the workshop and the actions being taken by the AAO.

Background

The 2006 review of the AAO recommended that the AAT should continue to operate for at least 10 years and that a new instrument is needed to keep it internationally competitive. The Australian government has provided $5.9M specifically for a new AAT instrument through the NCRIS scheme.

The development of concepts for the new instrument has been proceeding for some time. The AAO has polled the community for their views via the AAOUC and workshops, and it has developed the science and technical cases for a number of instrument concepts. This workshop provides the community with an opportunity to compare the science cases and consider the technical concepts being proposed.

The purpose of this workshop is to review the various concepts and rank them based on a judicious balance of (i) scientific merit: both impact of major applications and breadth of science relative to the strengths of the Australian community and complementarity or synergy with other facilities; (ii) technical merit: feasibility of implementation, breadth of capability, long-term strategic value; (iii) cost and performance: affordability, value for money.

One area of uncertainty in planning for the new AAT instrument is the outcome of the Aspen process, and in particular whether WFMOS will be built for Gemini and Subaru. The WFMOS concept studies will be reviewed in March 2009, but a decision on the new AAT instrument must be made sooner, to allow the AAO to begin work as soon as possible. The community thus has to make the best decision for the AAT without knowing what decision Gemini may make.

The available resources for the new instrument are also somewhat uncertain: the AAO has $5.9M from NCRIS but does not yet know the level of its recurrent funding in future years. Based on current information, a reasonable estimate for the available funding is ~$9M over 3–5 years.

AAOmicron

AAOmicron is a near-infrared (NIR) multi-object spectrograph (MOS) that utilises the existing 2dF corrector and fibre positioner. It would have ~240 fibres over a 2-degree field of view and cover the wavelength range from 0.9μm to 1.7μm (i.e. zJH bands) at a resolution R~3500–4000; the expected total system throughput is 10–15%. It can be thought of as extending 2dF/AAOmega with a NIR channel. The estimated cost of AAOmicron is $8M (assuming the AAOmega camera design can be used with minor modifications); the estimated construction period is 4 years.

The main science case is focussed on z=1–2 galaxy populations and their evolution. There was some doubt expressed as to whether AAOmicron on the AAT is capable of observing Hα in galaxies at z~1 as proposed, though performance modelling suggests this is feasible. AAOmicron would also be applicable to the study of low-mass stars, for which NIR spectroscopy is essential.

The overall consensus was that AAOmicron probably had the least strong science case of the instruments considered, although it is sufficiently different to the existing suite of instruments that this might to some extent reflect the community's lack of experience with NIR MOS.

Serious concerns were raised that the competition with FMOS severely weakens the case for AAOmicron. FMOS on the Subaru 8m telescope is comparable or superior in most respects: 400 fibres and R~500 or 3000, with OH suppression and probably a 4-year head-start, although it only has a 30 arcmin field of view. FMOS may therefore clean up the headline science in this area before AAOmicron could be built. AAOmicron's advantages relative to FMOS are its 16x larger FoV (hence a 4x AΩ gain for surveys) and the availability of more time.

HERMES

HERMES is a High-Resolution Multi-object Echelle Spectrograph. It uses the 2dF corrector and fibre positioner to observe 400 (perhaps 540) objects simul-

taneously over a 2-degree field at a resolving power R~30,000. The current concept covers a total of 400Å anywhere in the visible range from 0.37μm to 0.95μm. HERMES should be able to reach S/ N=100 in 60 minutes at V~14. HERMES can be thought of as extending 2dF/AAOmega to higher spectral resolution. The estimated cost of HERMES is ~$8.5M and the estimated construction time is 4 years.

The primary science driver for HERMES is 'Galactic archaeology' – the study of the dynamical and chemical structure of the Galaxy in order to understand its formation. There was a clear consensus that this was the strongest and most original science case for any of the instruments. It is also a unique area of discovery space (RAVE does not have the resolution for detailed chemical abundances). The practical limit at this resolution on a 4m telescope would be V~15, but this is well-matched to following up GAIA, a very powerful combination. To broaden the science applications and user base of a big Galactic archaeology survey, the 6dFGS strategy of calling for proposals for secondary targets that could use any spare fibres could be adopted.

Aside from the primary science case and variations (stellar radial velocities and abundances – i.e. dynamics and chemistry), HERMES has applications to 'PI' studies of the LMC, bulge and outer Galaxy, and more specialized studies of (e.g.) the lithium abundance and the ISM. A workshop at the AAO on 26 February 2008 will look at other science applications of HERMES.

There are few other high-resolution, multi-object spectrographs. In fact only Hectochelle on the MMT would appear to offer direct competition. (1-degree field of view, 250 fibres, R~30,000, already in use). HERMES offers 4x the field of view, 2x the multiplex and 2x the spectral coverage of Hectochelle, as well as access to the southern hemisphere.

WFMOS-A

WFMOS-A is an AAT version of the Wide-Field Multi-Object Spectrograph (WFMOS) proposed for Gemini/ Subaru. It uses the 2dF corrector optics (though possibly with a modification to the final elements of the corrector) but replaces the 2dF fibre positioner with an Echidna-style positioner having a 5–10 minute reconfiguration time.

The baseline version of WFMOS-A has 1600 fibres (4x AAOmega) and uses the two AAOmega cameras plus a duplicate to give a 3-channel, single-beam (i.e. half the simultaneous wavelength coverage of AAOmega), low-resolution-only system costing ~$15M and taking 4–5 years to build.

The optimal version of WFMOS-A has 1600 fibres feeding 3 dual-beam AAOmega spectrographs (i.e. 6 cameras giving the same simultaneous spectral coverage as AAOmega). It should include modified corrector optics (costing ~$1M) to maintain the current AAOmega throughput (as the non-telecentricity of the current corrector gives inefficient coupling to the Echidna spines). However this version is also low-resolution only and costs ~$18M, with a 5-year build time.

Other possible upgrades to the optimal version include: (i) implementing the HERMES spectrographs, giving high-resolution as well as low-resolution capability; 3 HERMES spectrographs would cost an additional ~$7M (i.e. a total of ~$25M) and take ~5 years. Note, however, that there is a mismatch between the sparse sky sampling of the Echidna positioner and the efficient use of the full 2-degree field for relatively shallow stellar surveys;
(ii) implementing up to 2500 fibres, requiring 5 AAOmega and 5 HERMES spectrographs; this would cost an additional ~$13M (i.e. a total of ~$31M) and take ~6 years.

The primary drivers for the WFMOS-A low-resolution science were large-scale galaxy surveys, particularly surveys aimed at measuring the baryon acoustic oscillations to study the dark energy equation of state. A z~1 million-galaxy survey over thousands of square degrees would reduce the current uncertainties on the equation of state parameters by substantial factors. There are, however, many other programs also proposing large BAO surveys, including the Gemini/Subaru version of WFMOS, the BOSS survey on the SDSS telescope, and the VIRUS survey on HET.

There was a strong preference for the optimal version over the baseline version (significant gain in capability for modest increase in cost); however there was also a general consensus that the additional upgrades to include HERMES or more fibres were probably unrealistically expensive.

Opinions were divided on whether the factor of 4 represented by the 1600-fibre versions of WFMOS-A relative to AAOmega was significant or incremental – in principle AAOmega could do the WFMOS-A science with 4x as much telescope time (starting now rather than in 5 years' time). However it was agreed that WFMOS-A was the single new instrument with the broadest range of scientific applications (both dark- and bright-time), including a lot of 'PI' science (i.e. all the science being done with AAOmega together with more ambitious programs). On the other hand, AAOmega plus HERMES is arguably at least as broad.

The overall cost of WFMOS-A (at least twice as much

as the other instruments) is a major concern. It would require finding a partner to share the cost. A 50% contribution to the cost of construction (say ~$9M) might buy 15–20% of the time on the AAT over 5 years. The strong preference not to cede scientific leadership to any partner may limit the funding to the optimal low-resolution version.

NG1dF

NG1dF is a high-multiplex imaging slit spectrograph for the prime focus of the AAT, proposed by Tom Shanks and Robert Content. The concept for NG1dF is at an earlier stage of development than the other instrument concepts. It is intended to provide low-to-moderate resolution spectra for thousands of targets over the 1º field provided by the (decommissioned) WFI prime focus. It is a cheaper and easier de-scope of the original NG2dF concept (Content & Shanks), which proposed using the 2dF top-end. NG1dF is in part stimulated by the IMACS/ PRIMUS instrument at Magellan, which provides very low resolution (R~40) slit spectra for many targets (~5000) over a 25 arcmin field. NG1dF would use 4 cloned spectrographs to observe ~4000 objects simultaneously at R~400 over a 2000Å spectral range. The cost of NG1dF has not yet been reliably estimated, but it would likely fit within the currently available funding.

The primary science case is based on very large galaxy surveys at moderate redshifts. For example, NG1dF might be able to measure 250,000 z~0.7 galaxy redshifts in 10 nights (i.e. the 2dFGRS at 6x higher redshift and ~4 mag fainter in just 5% of the observing time). It is partly driven by the upcoming availability of large-area deep imaging surveys (e.g. SDSS, SkyMapper, VST Atlas, Pan-STARRS, VISTA, LSST). It may also be suited to following up the next generation of radio surveys (e.g. ASKAP HI and continuum surveys). Rough estimates of the depths achievable with 1-hour exposures in 2 arcsec seeing are: (i) i<22 galaxy redshifts at z~0.7 from [OII]3727 at S/N>6 (target density ~5000deg^{-2}); (ii) i<21 galaxy redshifts from absorption lines at S/N>4 (target density ~2500deg^{-2}).

A major galaxy survey with NG1dF might have the following parameters: 4000 galaxy redshifts per hour including 3000 z~0.7 [OII] emission galaxies with 21<i<22 and 1000 z~0.5 absorption and emission galaxies with i<21. In 200 nights this would give 4 million z~0.7 galaxies and 1 million z~0.5 galaxies for a total of 5 million z<1 galaxies over 1600deg^2. In the best seeing (~1 arcsec) NG1dF could also observe z~3 r<25 LBGs, taking 4x3hrs to get 4000 redshifts; so in 20 nights (10% best time) it could also get 40,000 LBGs at z=3 over 10deg^2 or 0.4Gpc^3.

Other science that could be pursued with NG1dF includes: studies of galaxy properties and their inter-relations as functions of redshift and environment; mass mapping of clusters (together with weak lensing); photometric redshift calibration for SNAP, LSST, etc.; a legacy spectroscopic archive of the southern sky; also 'needle in a haystack' surveys for rare objects such as high-z QSOs and brown dwarfs. If the instrument provided 1–2Å resolution over 200Å (i.e. R~4000 as well as R~400) then it would be useful for a wider range of science programs.

The primary science case is interesting, but, as currently conceived, NG1dF has 3x lower spectral resolution and less than 1/2 the spectral range of AAOmega or (optimal) WFMOS-A, which limits to some extent what it can do, both in terms of redshift range covered and more detailed physical studies. Consequently the breadth of the science supported by NG1dF is significantly less than for WFMOS-A (though perhaps comparable to HERMES); however NG1dF would be a good complement to AAOmega. Competition for NG1dF comes from wide-field multi-slit spectrographs such as VIMOS, IMACS/ PRIMUS (especially with higher resolution grism). These have 0.5 deg fields but are on larger telescopes.

Other Issues

Maintainability of 2dF: If AAOmicron or HERMES were chosen as the next AAT instrument, then the maintainability of the 2dF positioner over their lifetime has to be considered. With suitable ongoing maintenance and perhaps one substantial refurbishment, the 2dF positioner can probably be supported for another decade. A possible alternative to a major refurbishment of the existing positioner would be a new Starbugs positioner.

Support for software and science: For any of these instruments, a major effort is needed on software support for (primary) science as well as software for data reduction and survey databases. There was also a plea for support of science personnel in order to fully exploit the science from the main programs (big surveys are always manpower-limited).

International partnerships: Some implementations of the proposed instruments (especially WFMOS-A, but also combinations of instruments) require substantially more funds than are currently available. It was a general and strongly-held opinion that the overseas share of any instrument should be at most 50%, and that Australia should retain the scientific leadership of the main programs. Nonetheless, it was also recognised that collaborations can be highly beneficial, especially in terms

of input target catalogues, data reduction and the publication of results. Collaborators would need to be carefully chosen for strategic purposes (e.g. access to large imaging surveys) and to ensure compatibility of science capabilities and goals.

Conclusions & Actions

AAOmicron: AAO will not develop the AAOmicron concept further at this stage, although it will complete the documentation of the work done to date and attempt to broaden the science case, in particular with regards to any areas where AAOmicron will have a clear advantage over FMOS. AAO will monitor the performance of FMOS when it is commissioned early in 2008.

HERMES: By general consensus, this instrument was the clear front-runner with the currently available funding, and the AAO will therefore focus its efforts on developing this instrument concept. The science case needs further work to refine the science requirements for the Galactic archaeology program, and to broaden the case as much as possible. In addition, the AAO will undertake further investigation of the work and costs involved in maintaining the 2dF positioner for another decade.

WFMOS-A: The AAO will complete the WFMOS-A concept study early in 2008; it will then focus solely on the Gemini WFMOS concept study that will be starting in early 2008, and which will be reviewed by Gemini in March 2009. After the WFMOS-A concept study is completed, no further development of WFMOS-A will take place unless the Gemini instrument is cancelled, in which case WFMOS-A might be reconsidered as a potential fallback option for some subset of the Gemini/Subaru partnership.

NG1dF: The NG1dF concept was considered an interesting dark-time instrument option, though ranked below HERMES. However there needs to be substantial development of the science case, technical design and costing before it could be taken further. The AAO will carry out a preliminary joint study with the University of Durham. NG1dF is likely to cost substantially less than WFMOS-A, and it may therefore be a more realistic option for an international collaborative venture. There was considerable interest in seeing whether the existing funding could be leveraged to implement both HERMES and NG1dF.

IMPROVED PRECISION OF 2DF FIBRE POSITIONING

Russell Cannon, Tony Farrell, Will Saunders, Rob Sharp and Scott Croom

The 2dF positioner problem

Although the 2dF robot has an internal measuring accuracy of a few microns and is required to place fibres to within 15μm of specified positions, observers have often noticed that some of the 2" diameter fibres miss their targets, implying positioning errors of ~100μm or more. In effect, the robot was placing fibres very precisely but in the wrong positions. Numerous improvements to the hardware, software and observing procedures have helped to reduce these errors since 2dF was commissioned in 1996, but when the much-improved AAOmega spectrographs (Smith et al. 2004, Saunders et al. 2004) were commissioned in 2006 it was still clear that fibres in some regions of the field were being systematically misplaced, resulting in unusable spectra for a small percentage of targets and an overall loss of observing efficiency of as much as 20%. (Sharp et al. 2006).

The astrometric errors were not a serious limitation for determining the redshifts of the relatively large and bright galaxies in the original 2dF Galaxy Redshift Survey (Colless et al. 2001). However, the losses were more significant for QSO surveys, for subsequent galaxy surveys at higher redshift, and of course for all stellar projects. Many projects with the new AAOmega spectrographs require uniform target coverage and high signal-to-noise ratio spectra for ever fainter targets.

In this note we report on several recent improvements to the calibration of 2dF and changes to the configuration software. These have led to a substantial gain in the precision with which fibres are positioned. All 400 fibres are normally now placed to better than 0.25" rms across the full field. As well as increasing overall observing efficiency and the uniformity of AAOmega data, this enables longer total observation times without reconfiguring and should permit first-order corrections for varying spectral response.

How 2dF works

The 2dF instrument has two interchangeable field plates mounted back-to-back and two large XY gantries, the upper Gripper gantry which carries the robot that positions the magnetic buttons at the ends of the fibres and the FPI gantry which faces the primary mirror of the AAT and carries the Focal Plane Imager. Both gantries are fitted with CCTV cameras that can look at back-illuminated fibres. The 2dF software converts the

positions of targets and guide stars (in celestial coordinates) to XY coordinates in the focal plane, taking account of many known factors such as atmospheric refraction and optical distortion in the 2dF corrector lens.

Sets of astrometric standard stars are measured with the FPI and used to determine the transformations between calculated star positions and the 2dF XY scales. This is known as the "poscheck" procedure and is carried out every time 2dF is put on the telescope. The basic reference frame is provided by a set of 21 illuminated fiducial pinholes in each of the field plates (the coordinate system is thus different for the two plates). The same fiducial pinholes are measured by the positioner gantry after the two field plates have been interchanged by the tumbler, thereby completing the transformation between input positions on the sky and robot coordinates. Each successive XY transformation is calculated by a linear least squares fit, allowing for zero point shifts, rotation, skewness of axes and scale changes.

There are many potential sources of astrometric errors and many parameters needed to define the coordinate transformations. It gradually became apparent that some errors are insignificant in practice while others were not foreseen at all. Some parameters which were treated as unknown variables can be fixed, improving the definition of those parameters which do vary. Mechanical flexure effects are generally very small, which made it unnecessary to take many "poschecks" at different declinations at the start of each 2dF run. Unforeseen problems include the non-straightness of some gantry axes, making linear coordinate transformations inadequate, and spurious distortions of the coordinate system when some fiducial pinholes are occulted by fibres.

The overall performance of 2dF has been greatly improved by recent improvements to the hardware, especially the installation of much flatter field plates in 2005, the provision of 8 rather than 4 guide star bundles as part of the AAOmega upgrades in 2006, and the fitting of a new gripper jaw mechanism, designed and fabricated by Rob Patterson at the AAT, in October 2007.

By 2006 there were three remaining major astrometric problems: (i) unknown distortions of the XY axes, especially in the Gripper Gantry; (ii) errors arising from using only subsets of the plate fiducials; and (iii) the unknown offset of the optical axis of the corrector lens. Several special techniques were devised to tackle these problems.

Mapping the relative distortion of the Gripper and FPI gantries

The relative distortion between the two 2dF gantries can be mapped by configuring the 2dF fibres in a rectangular grid pattern and measuring the positions of the back-illuminated fibres. It may seem strange to measure deformations of the axes using a configuration which has been set up by the Gripper gantry itself, but all we are looking for are the differences in the measured positions: the absolute accuracy of the positioning is not important. Fig. 1 shows the results of one such test, with greatly magnified vectors showing the residual shifts

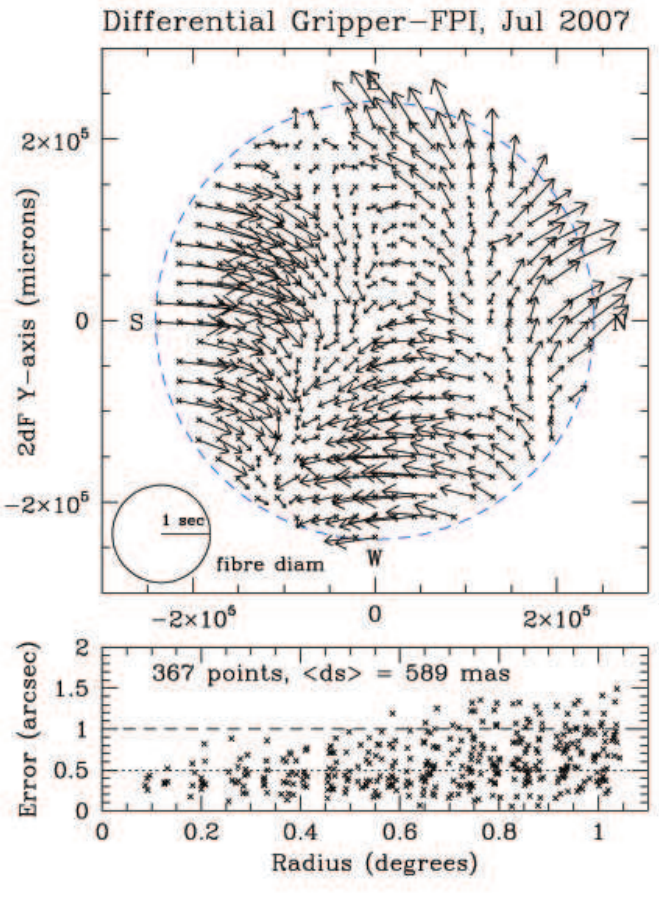

Figure 1: The differential distortion between the FPI and Gripper gantries, as determined from a back-illuminated rectangular grid configuration of fibres.

of the buttons as seen by the two gantries. The circle in the lower left hand corner represents a fibre diameter on the same scale. These are the residuals after applying a best-fit linear transformation to the two sets of encoder counts. There are clearly systematic non-linear distortions across the field, with some residuals larger than 1". The lower panel in Fig. 1 shows the sizes of the residuals as a function of radial distance from the field centre.

Clearly there are substantial errors in the XY coordinate systems of one or both gantries. The Gripper gantry was the main suspect. Direct tests against a straight-edge had shown substantial curvature of some of the rails, while the gripper head is heavy and presumably more prone to tilt of the Z-axis. No simple analytic function can fit the pattern of distortion seen in Fig. 1, so a correction map was derived by combining the results of several such tests, with some smoothing and interpolation for missing grid points. Differential gantry corrections have been applied since July 2007 and produced a significant improvement in the accuracy of fibre positioning, as judged from the acquisition of guide stars and from reduced scatter in plots of total signal versus expected magnitude of targets. However, significant errors remained.

The relative distortion of the gantries also turns out to be the underlying cause of the plate fiducial problem. In theory, a few fiducials should be adequate to define the location of the rigid 2dF field plates. However, it became apparent that the coordinate transformations were rather unstable and depended on which fiducials were measured. Evidently the two gantries did not see the pinholes in the same relative positions. The solution was to allow for these differences empirically. It had been assumed that the problem arose in the optics of the two CCTVs, but the differences virtually disappear when the differential gantry distortion map is applied to the fiducial measurements.

The same grid configurations of fibres can be used to check for flexure effects between components of 2dF, by slewing the telescope to extreme positions in hour angle and declination and re-measuring the back-illuminated fibres. Most such effects turn out to be reassuringly small and in fact the FPI gantry has negligible distortion. The Gripper gantry occasionally shows shifts of a few microns, probably because the gripper assembly is heavier than the FPI, but about the only correction which might be worth applying is a small sag of about 15μ in the Y-beam of the Gripper gantry at extreme declinations.

Another special configuration can be used to measure the differential curvature of the gantry axes directly, by

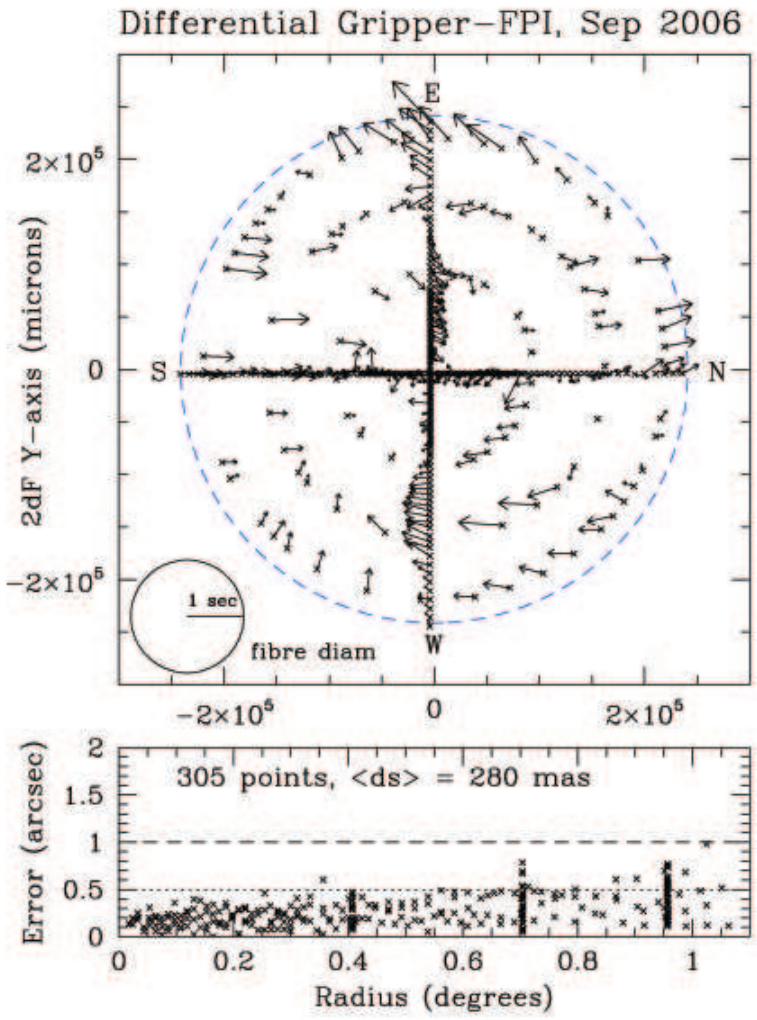

Figure 2: The relative curvature of the gantry axes, as determined from a cross-shaped configuration of back-illuminated fibres.

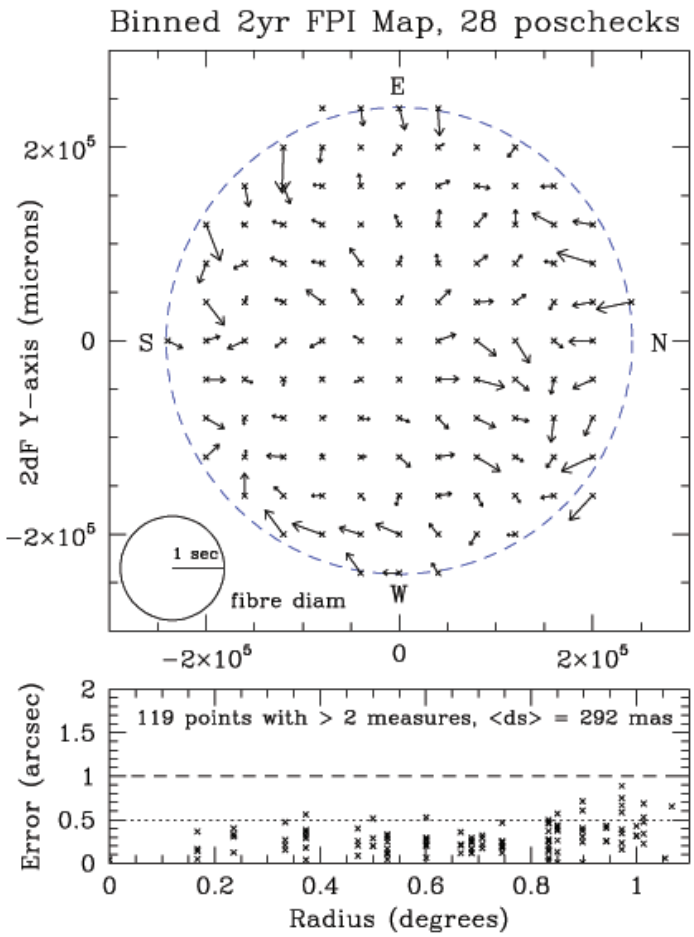

Figure 3: Residual distortions due to the FPI gantry and/or the 2dF corrector lens optics, using the binned data from over 2200 "poscheck" stars.

placing as many fibres as possible along the X and Y axes. Spare fibres were placed in three concentric rings. Fig. 2 shows the result of comparing the positions as measured by the FPI and Gripper gantries. The X axes have the same shape, but large scale relative curvature of the Y axes with an amplitude of around 30μm is evident, consistent with the earlier straight-edge tests.

The FPI gantry distortion as measured from "poschecks"

In principle, the absolute distortion of the FPI gantry can be determined by measuring standard stars. The routine "poscheck" measures done at the start of each 2dF run already provide such data. However, there are two problems: the astrometric precision of each single star measurement is low because the exposures are typically only around 1 sec, and the measurements have to be done sequentially and are thus subject to telescope tracking errors. The result is that the rms scatter in a set of ~80 Tycho stars is typically around 50μm. Such errors are too high, and the density of points too low, to reveal systematic distortions. However, the long-term stability of many of the 2dF astrometric parameters means that it is now feasible to re-analyse the original data and to combine many poschecks taken over several years, in order to increase the number of stars and lower the errors.

Such an FPI map will of course include any systematic optical distortions introduced by the 2dF corrector lens, and in particular the previously very uncertain location of the optical axis relative to the field centre. The radial distortion of the 2dF field can be modelled by a polynomial in the radius, with odd terms up to the 7th order. An error of 1mm in the assumed centre will cause image shifts of 1" at opposite edges of the field.

The result of combining the data for 2275 stars from 28 good sets of "poscheck" data taken in 2006 and 2007 is shown in Fig. 3. The data have been binned in a rectan-

gular 13 × 13 grid with an average of 19 stars per bin. A best-fit correction for the offset of the optical axis has been applied, after checking that the same correction was valid for the data from both years separately. Clearly any systematic distortions arising in the FPI gantry or the optics are small compared with the differential distortions shown in Fig. 1: the earlier assumption that most of those errors arise in the Gripper gantry was justified. While the vectors in the FPI map are relatively small, with an rms of 0.3" or about 20μm, they are not negligible. There is real large-scale structure in Fig. 3, as shown by the correlated errors in adjacent but independent boxes. Moreover, the patterns for 2006 and 2007 analysed separately are very similar, although both have larger random errors. A smoothed version of Fig. 3 has been used to derive an FPI correction map, which is applied to the calculated target positions in the same way as the differential Gripper-FPI map based on Fig. 1.

Raster scans as an overall system check

The ultimate test of 2dF positioning accuracy is to configure a field of standard stars and determine the offsets of the fibres relative to the centroids of the star images. This is achieved by carrying out a raster scan, typically a series of short exposures in a 3 × 3 rectangular grid pattern with 1.5" spacing. The fibre offsets can then be determined from the relative counts in the nine exposures.

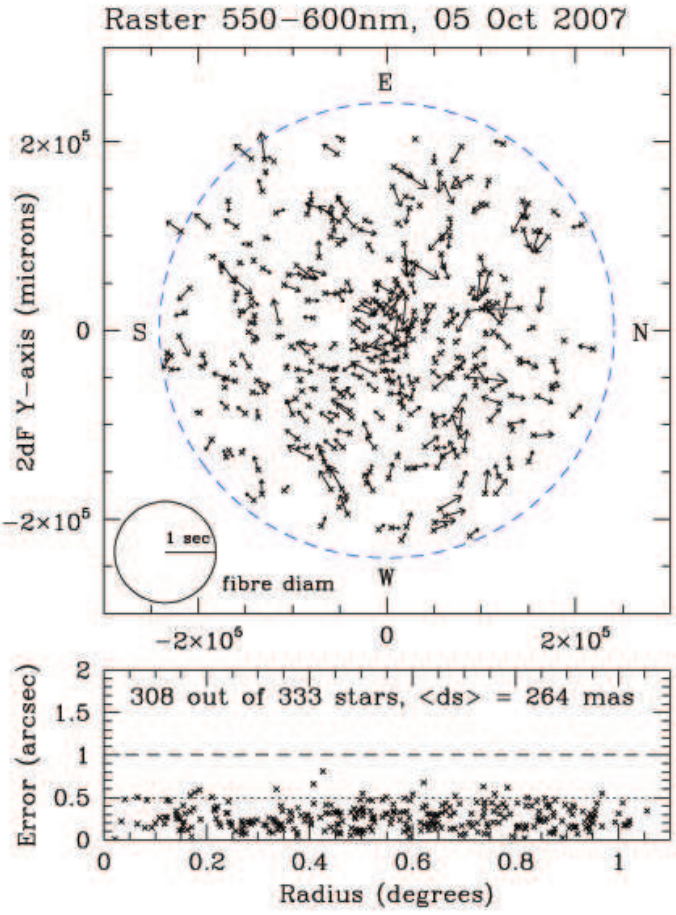

Figure 4: The overall precision of 2dF positions, as determined from a raster pattern of exposures on a set of astrometric standards. The vectors show the offsets of the fibres relative to the star image centroids.

Fig. 4 shows the results of one such raster scan, done in October 2007 after various changes described above had been implemented. It was immediately clear that the basic astrometric problem had been solved, with virtually all targets appearing brightest in the central exposure of the raster pattern. The stars were taken from the UCAC2 astrometric catalogue, which provides a high enough density of targets. Small shift and rotation corrections have been applied, to mimic the effect of guiding in normal observations, and the faintest 25 targets have been omitted to reduce the scatter in the derived centroids. The overall mean error in the positions is only 0.27", with very few offsets larger than 0.5". The rms errors in X and Y are 14μm or 0.2", finally reaching the original 2dF specification.

There was one extra detail in the above analysis. The scales in both coordinates were changed by a factor of 1.0001, to remove a small systematic radial trend apparent in the vectors. This correction amounted to 25μ at the edge of the field, small compared with previous errors, and produced a 35% decrease in the scatter. Such a scale change could be due to a 5°C change in temperature. One further refinement to the 2dF configuration procedure will be to include a temperature term in the plate scales.

Other effects can be investigated using the same raster scan data. For example, substantial Chromatic Variation in Distortion (CVD) is predicted across the 2dF field, due to the corrector lens design.[1] This means that while the light at all wavelengths coincides at the centre of the field and again at the edges, there are substantial

[1] http://www.aao.gov.au/AAO/2df/aaomega/aaomega_CVD.html

radial shifts at intermediate radii. Fig. 5 shows the result of comparing image centroids in bands centred at 525nm and 850nm. The positional shifts amount to 0.6" at a radius of 0.6°. The thick dashed line in the lower panel shows the expected result from the design parameters of the 2dF corrector. The overall shape is very close to what was predicted although the amplitude had to be decreased by 20% to fit, probably because a rather crude Centre-of-Gravity algorithm was used to derive the observed centroids.

Future improvements, possibilities and limitations

Now that the basic astrometric performance of the 2dF robot is within specification, there is scope for various further improvements. For example, it will be worth implementing small but significant corrections for flexure of the gantry Y-beams and for the temperature dependence of the plate scales. Tests are planned in the coming months to determine whether there are flexure shifts in the optical axis of the corrector as the AAT is slewed across the sky: the current offset was determined from observations close to the zenith. The performance of the Atmospheric Dispersion Compensator (ADC) can be checked, in case the counter-rotating components introduce some field distortion.

With the positioning errors now smaller than the effects of CVD (Fig. 5), it should be possible to apply at least first-order corrections to the instrumental response and improve the flux calibration of AAOmega spectra, usually one of the weakest features of fibre spectra.

The total time that a given 2dF configuration can be observed is limited by the effects of atmospheric refraction, and decreases rapidly with increasing zenith distance. As a by-product of these astrometric investigations, it was realised that the exposure time guidelines specified for 2dF are too stringent. Standard procedure has been to configure each field for the mid-point of the planned exposures, and if possible to have the field crossing the meridian at that time. In fact, it is better to use a mean configuration, which may never match the actual pattern on the sky precisely, and a substantial component of the field distortion can often be removed by rotating the field plates. These changes are now being implemented in "configure" and should lead to a doubling of the maximum efficient observing times in some circumstances.

Further details on AAOmega observing may be found at:

http://www.aao.gov.au/AAO/2df/aaomega/aaomega_preps.html

References

Colless, M. et al., 2001, MNRAS, 328, 1039
Saunders et al., 2004, SPIE, 5492, 389
Sharp et al., 2006, SPIE, 6269E, 14, arXiv:astro-ph/0606137
Smith et al., 2004, SPIE, 5492, 410

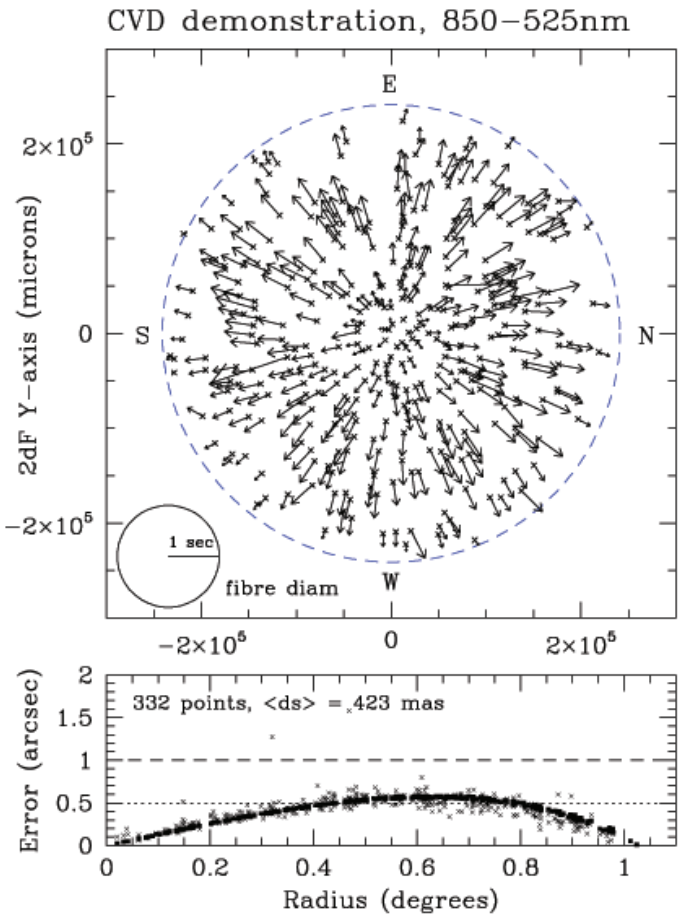

Figure 5: A demonstration of the Chromatic Variation of Distortion in the 2dF corrector lens at two different wavelengths. The solid points in the lower panel compare the predicted effect as derived from the optical design parameters.

ASTRONOMY AND RITUAL WARFARE IN ANCIENT PERU

Fred Watson

Perhaps more than most folk in today's world, astronomers are tuned in to the idea that ancient cultures placed great significance on the things they saw in the sky. Often, as in the case of the indigenous people of Australia, the legends associated with the sky had a practical purpose. For example, they defined seasons when it was worthwhile hunting for a particular food – berries or insect larvae – and, in other cultures, when it was the right time to plant crops.

In the coastal deserts of Peru, human settlement clung to the floodplains of Andean rivers, which still cut a green swathe through the pale grey-brown of the desert soil. Water meant everything, and the ebb and flow of the rivers – which in reality is determined by distant snowmelt – was believed to be controlled by supernatural beings. These were the ancestor-gods, or *huacas*, who were considered by many ancient Peruvian cultures to intervene directly in everyday affairs, and who were closely linked with the phenomena of the sky.

Astronomy and ritual

What happened when these gods disagreed among themselves? They would fight battles, and maybe the outcomes of those battles would determine who in the human world got water, and who didn't. But in the belief system of many ancient Andean people, a supernatural battle would have its parallel on earth, in the form of a ritual battle founded on religious belief – a holy war.

To initiate a ritual war, so the theory went, the *huacas* would speak to the leaders of their respective communities in dreams, or through astronomical phenomena. Thus, a belief in such messages was fundamental to the process, and clearly astronomical observations could have serious consequences in initiating battles with rival communities. Fortunately, today's astronomers don't have to worry about such outcomes, except in the mildest possible way.

At Chankillo, in the Casma valley in northern Peru, there is a site that is now known to have been the ceremonial setting for such ritual battles. Set high on a hilltop overlooking the main archaeological complex (which itself covers an area of some four square kilometres) is its most substantial and prominent feature. This imposing construction consists of two roofless circular buildings some 40 m in diameter with a third rectangular building of similar size close by. The three structures are all erected on an earthwork platform and surrounded by two rough stone walls, approximately triangular in plan, and massively built – up to 8 m high and 6.5 m thick.

It is principally from wooden lintels in doorways piercing these walls that the structure has been carbon-dated to the fourth century B.C. The site also shows evidence of damage due to seismic activity, which produces characteristic triangular breaks in the masonry. Peru, of course, is no stranger to earthquakes.

Thanks to the work of Iván Ghezzi, former Archaeology Director of Peru's Instituto Nacional de Cultura, this structure is now recognised as a fortified temple, with both ceremonial and limited defensive functions. It had an 'inner sanctum', the so-called Temple of the Pillars, which could be seen from almost anywhere in the district. The temple aligned with the summer solstice sunrise, and this alignment is maintained in the remnants of other buildings that stretch away two kilometres and more to the east.

There is evidence that the period of occupation of this building – and perhaps the whole site – ended suddenly in ritual warfare. On the hillside and the plain below it, thousands of round stones of a uniform size have been found. They are slingstones, which would have been gathered from the riverbed two kilometres away. In the hands of warriors, they would have been lethal weapons.

Figure 1: Looking decidedly unwell, a 3,300-year-old participant in ritual warfare decorates the mural wall at Sechín, near Chankillo. Note his long thumbnails, which are handy for gouging out the eyes of enemies. Ritual warfare, while limited in its scope, was barbaric in its practices. (*Fred Watson*)

Figure 2: The shattered remains of the Temple of the Pillars at Chankillo. The long axis of the building (across the photo) aligns with the summer solstice sunrise. (*Fred Watson*)

One particular room in the Temple of the Pillars shows evidence of having been systematically destroyed. A thick layer of dirt and stone has been piled into it in a manner quite different from the damage caused naturally by earthquakes. Indeed most of the stony material is of a type not found at Chankillo, and it must have been transported from elsewhere. It is as if the intention was to annihilate this room completely. Along with whatever gods and altars it had housed, it was meant to be eradicated from memory altogether.

It was presumably the threat of such ritual destruction that justified the building of such a remarkable structure, which could have had no role in the protection of settlements, agriculture or water sources in the area. For the astronomers of Chankillo, too, the same threat would have been the motivation for their observations. And today, we have spectacular evidence of that in the form of a unique row of square towers running along a barren hilltop.

Thirteen towers

In March 2007, Iván Ghezzi and his collaborator, Clive Ruggles of Leicester University, made world-wide headlines with their announcement that the mysterious Thirteen Towers of Chankillo constitute a previously unrecognised solar observatory, some 2,300 years old. Seven months later, I wrote to these two scientists, explaining that I was about to bring a party of interested Australians on a study tour of the ancient astronomical sites of Peru – and that we would be starting with Chankillo. To my delight, Iván offered to accompany us on our visit, and his presence provided extraordinary insights into the minds of the site's builders.

What are these Thirteen Towers? And why are they so significant? In the desert to the east of the hilltop temple-fortress described earlier are many archaeological remains. Foundations of gigantic rectangular structures, clearly visible on satellite imagery, litter the desert floor. These are the remnants of buildings and plazas, the main fabric of the ceremonial complex of Chankillo. Running northwards through the middle of the complex is a line of low hills, and the northernmost one – a prominent ridge rising some tens of metres above its surroundings – is surmounted by a row of thirteen square towers. Their solid stonework construction and regular spacing (of about five metres from one tower to the next), together with the provision of a pair of staircases running up each tower, speak of an important purpose whose identity has, until now, remained a mystery.

The 200 m long line of towers runs almost exactly north-south, although there is a well-defined bend in the alignment of the three southernmost towers. They twist

Figure 3: The Thirteen Towers of Chankillo run along a narrow north-south ridge. Despite the effect of earthquakes throughout their 2,300 year history, each tower still has two staircases like the one seen here at the northern end of the row. (*Fred Watson*)

Figure 4: Although only eleven of the thirteen towers are visible from the eastern observation point identified by Iván Ghezzi and Clive Ruggles, their purpose is clear. They provide an artificial skyline graduated to mark the position of the setting Sun. (*Rob Hollow*)

around to the southwest, following the line of the ridge. From points to the east or west of the towers, observers are presented with the extraordinary spectacle of a skyline punctuated by a series of regularly-spaced notches – formed by the gaps between the towers. This suggested to Ghezzi and Ruggles that the towers had some astronomical significance, and their subsequent research has borne this out.

What these scientists have done is to identify two significant points among the low-lying ruins of the complex where observations of the rising and setting Sun could be made. On the western side of the towers (where sunrises would be observed), this is the open end of a long corridor, whose walls would originally have been more than two metres high. Thus a doorway at the end of the corridor would have faced the line of towers, some 235 m away. On the eastern side (corresponding to sunset observations), there are the remains of a small building some six metres square, which also seems to have had an open doorway.

These two doorways define an east-west line that bisects the line of towers. Ghezzi and Ruggles note that viewed from either of them, the row of towers corresponds in length to the range of azimuths that the rising and setting Sun would adopt throughout the year, calculated for 300 B.C. Thus, at any time of the year, the rising or setting Sun could be observed, and its alignment measured relative to the series of artificial notches along the hilltop. This would give an estimate of the time of year accurate to just a few days. It contrasts strongly with other Peruvian sites, in which only the sunrise and sunset positions at the solstices are marked.

The purpose of the line of towers was therefore to serve as a giant calendar, allowing the high priests of the community to dictate with certainty when crops should be planted, or when religious ceremonies should be enacted – or when ritual wars should be initiated.

Unanswered questions

Notwithstanding Ghezzi and Ruggles' careful reconstruction, there are still mysteries surrounding the thirteen towers. One is that their height varies systematically along the hilltop. We know from their structure that despite significant earthquake damage, the towers are the same height today as they were when they were built, so there is a strong impression that the varying height of the towers is quite deliberate. But why should that be the case?

Since the height of the towers increases towards the northern end of the row, they combine to effectively reduce the inclination of the artificial skyline compared with the natural line of the hilltop itself. This means the tops of the towers follow more closely a meridian of hour angle, so that the Sun would always cross them at the same time of day throughout the year (solar time, not mean time). It is far from certain, however, that this is the reason for the gradation.

Another mystery concerns the visibility of the towers themselves. Because of the westerly bend in the line of towers at its southern end, only eleven of them are seen from the eastern observation point. The other two are either on or below the local horizon. From the western side, all thirteen towers are visible. But there's a subtlety. If Ghezzi and Ruggles' identifications of the two observing points are correct, the eastern point is slightly closer to the line of towers than the western point, meaning that the towers still cover the full range of azimuths displayed by the setting Sun, even though two of them aren't visible.

Perhaps this was a natural way of compensating for the twist in the hilltop that hid the southernmost towers from view at sunset, but the builders could equally well have dealt with it by making the southernmost towers higher, keeping the eastern observation point at the same distance from the line as the western one. Is it too fanciful

to suggest that having the two observation points at different distances from the line provides additional information to an observer who watches both sunrise and sunset on the same day? Potentially, it would allow the astronomical calendar to be calibrated more finely, perhaps even allowing the exact day of the year to be determined – at least near the equinoxes, when the Sun is moving most rapidly.

Figure 5: From the hilltop temple-fortress a kilometre to the west, all thirteen towers can be seen. The sunrise observation point identified by Ghezzi and Ruggles is at the further end of the narrow corridor whose remains are in the lower right corner of the photo. (*Marnie Ogg*)

At the time of writing (February 2008), Ghezzi and Ruggles are planning further investigations of the eastern and western observation points at Chankillo, and may eventually reveal new insights into the functionality and use of the towers. Whatever the outcomes, there will certainly be no diminution of the almost magical aura that surrounds these remarkable structures.

In its small way, our study tour group also made history by becoming the first from Australia – and among the first in the world – to see the thirteen towers first-hand. And there's no doubt that our pilgrimage to this largely unvisited area of northern Peru has left an indelible mark on us all.

Acknowledgements

I am indebted to Iván Ghezzi for his generosity in welcoming a group of rank amateur archaeoastronomers into his world, and for giving us many valuable insights into the archaeology of Peru. It is also a great pleasure to thank my fellow members of the Peru expedition for their stimulating company on the trip, and Helen Sim for useful input during the planning stage. Finally, it was Marnie Ogg of Thrive Australia who proposed, arranged and ran the tour. Her professionalism facilitated a stunning trip that all the participants will remember with gratitude for the rest of their lives.

Figure 6: Participants in the archaeoastronomy tour attempt to reconstruct the Thirteen Towers of Chankillo in a local restaurant after the visit. (*Rob Hollow*)

Further reading

Ghezzi, Iván, 2006. 'Religious Warfare at Chankillo', in *Andean Archaeology III: North and South* (eds. W. Isbell and H. Silverman), Springer, New York, pp.67–84.

Ghezzi, Iván, and Ruggles, Clive, 2007. 'Chankillo: A 2300-Year-Old Solar Observatory in Coastal Peru', *Science*, Vol.315, pp.1239–1243.

Watson, Fred, 2008. 'When the Stones Speak: An Archaeoastronomy Tour of Peru', in *Yearbook of Astronomy, 2009* (eds. Patrick Moore and John Mason), in press, Macmillan, London.

UKST PLATE ARCHIVE MOVED TO COMPACT STORAGE

Russell Cannon (with thanks to Andy Longmore and Sue Tritton for input)

In May 2007 the main UK Schmidt Telescope Plate Archive was moved to a new location, still within the Blackford Hill premises of the Royal Observatory, Edinburgh. The UKST was established in 1973 as an independent Unit of the then SRC (later PPARC, now STFC), consisting of the telescope on Siding Spring Mountain and a base at ROE. All original UKST plates and films were stored in a large Plate Library at ROE, along with various inspection and measurement facilities. Control of the UKST itself passed to the AAO in 1988 and photography was gradually superseded by multi-fibre spectroscopy. Photographic work was discontinued in 2002, following the commissioning of 6dF in 2001.

All the main Sky Survey photographs (in the B, R and I bands, plus the H-alpha Atlas of the Milky Way) have been digitised, by SuperCOSMOS in Edinburgh and other machines, most good non-survey plates were analysed and most of the measuring machines have now been shut down. Nevertheless, the set of almost 18,000 photographs remains a unique record of the southern sky over the last quarter of the 20th century and contains much useful information on variable objects and transient events. For example, there are several requests per month to check the orbits of Near-Earth asteroids.

It was therefore decided to move all the original plates and films, plus glass copies of the Atlases, to a new much more compact storage area in the basement of the original 1894 Building at ROE. The move involved refurbishment of an area of the Observatory and this was funded by an allocation to the Astronomy Technology Centre (UKATC) from PPARC/STFC. PPARC/STFC also paid for the professional movers and for local support during this process (Sue Tritton, who for many years was primarily responsible for running the Plate Library). This should ensure the long-term safe storage of these legacy data, in a way that will still enable astronomers to access them when the need arises. A room close to the new archive has been refurbished as a “Plate Inspection Room”. This room contains light tables with microscopes, and a scanner for digitising regions of the plates may be added.

UKATC is responsible for appropriate maintenance of the storage facility and its environment. The University of Edinburgh’s Institute for Astronomy (IfA) has undertaken to support, at no extra cost, a low level of visitor access to the plates. If requests become greater than can be managed on a best efforts basis a more formal arrangement for support will need to be agreed by IfA with STFC. We want to ensure that this plate archive is as complete as possible, and urge any astronomers who still have any original UKST plates to arrange for their return to Edinburgh. Mike Read (mar@roe.ac.uk) is the primary contact person for anyone wishing to have access to the plates.

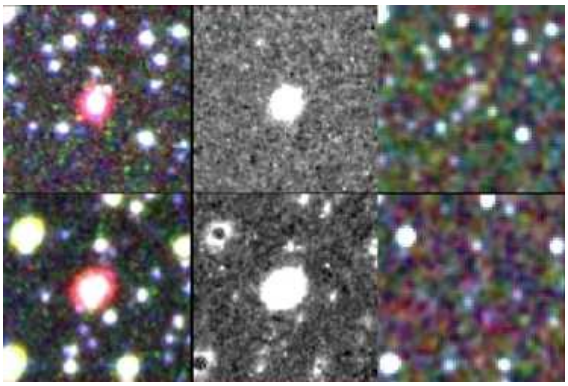

Exciting science is still being obtained from the UKST plates. Two compact MASH-II planetary nebulae (PNe) candidates, left to right, Hα, short-red and Bj composite, Hα/short-red quotient and 2MASS JHK stack. The lack of a 2MASS counterpart bodes well for the PN identification.

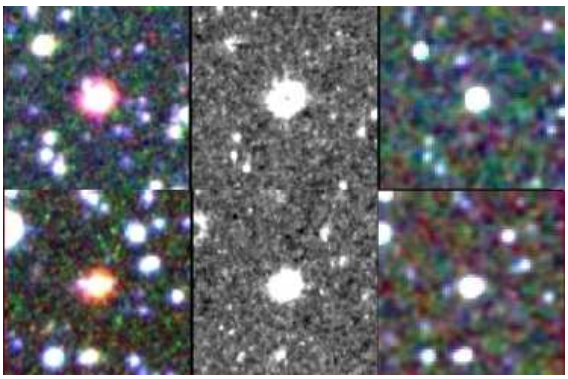

Additional compact MASH-II PN candidates. However, note that there is a bright 2MASS point source coincident with each of the putative PNe indicating that it is far more likely that they are stellar sources.

For further details of the significant Macquarie/AAO/Strasbourg H-alpha (MASH) discoveries of 250 additional new PNe (dubbed MASH-II) see the just published paper by Brent Miszalski, Quentin Parker and other MASH team members in Miszalski et al., 2008, MNRAS, 384, 525.

THE AAO WELCOMES THE AUSTRALIAN GEMINI OFFICE

Stuart Ryder (AAO)

Australia has a 6.2% share of time on the twin 8 metre telescopes on Mauna Kea in Hawaii and Cerro Pachon in Chile operated by the Gemini Observatory, amounting to approximately one week per telescope per semester. The Australian Gemini Office (AusGO) coordinates Australia's usage of Gemini time by issuing calls for proposals; acting as first point of contact for prospective Australian applicants; technically assessing proposals on behalf of the Australian Time Assignment Committee; assisting successful Australian Principal Investigators with preparing their queue-scheduled observing programs; providing guidance in how to reduce and analyse new and archival data from Gemini; and helping promote Australian science from Gemini to the media and general public. In addition, AusGO oversees aspects of Australian bids and contracts for Gemini instrumentation, such as the Near-infrared Integral Field Spectrograph (NIFS) and the Gemini South Adaptive Optics Imager (GSAOI) built by the ANU's Research School of Astronomy & Astrophysics (RSAA), and the AAO-led proposal for a Wide-Field Multi-Object Spectrograph (WFMOS). By a special arrangement with the Carnegie Observatories, AusGO is also facilitating Australian access to 30 nights on the twin Magellan 6.5m telescopes in Chile over Semesters 2007A–2008B.

AusGO has always been a "distributed office" in that it is managed by the Australian Gemini Scientist (AGS) for a 3 year term, assisted by two Deputy Gemini Scientists (DGS), each of whom would usually be located at a different institution from the AGS. In this way, Gemini expertise and visibility is better spread across the community than if all AusGO staff were concentrated in one location. AusGO also relies on some "honorary associates" to provide support for more specialised instruments. Both the National Collaborative Research Infrastructure Strategy (NCRIS) Investment Plan for Radio and Optical Astronomy, and the recent DEST review panel's report recommended that the AAO host AusGO for the 5 year timeframe of NCRIS funding, in line with the AAO taking on the role of Australia's national optical/infrared observatory. In January 2008, AusGO began the transition from RSAA to its new home within the AAO, where new offices on the ground floor of the Massey Building have recently been completed to accommodate the new staff.

In late 2007, an international recruitment and interview process was carried out to appoint the new AGS, and one DGS to be based at the AAO (a second DGS to be based at RSAA is currently being recruited). The new AGS for the period 2008–2010 is Dr Stuart Ryder, previously a Research Astronomer at the AAO. Since coming to the AAO in 1999, Stuart has been commissioning astronomer for IRIS2; instrument scientist for IRIS2, UCLES, and UHRF; and Technical Secretary to ATAC, PATT, and AATAC. Since 2001 Stuart has volunteered his services to AusGO as Contact Scientist for instruments including NIRI, Altair, bHROS, and Phoenix, and attended Gemini meetings in Vancouver, Tucson, and Iguassu Falls. Recruitment of a new Research Astronomer to fill Stuart's AAT-related roles for the next 3 years is currently underway.

The new AAO-based DGS will also be well-known to many AAT observers. Dr Terry Bridges was the AAO/UK 2dF Research Fellow from 1999–2003 before returning to his native Canada to work at Queens University in Kingston. Terry is a very experienced GMOS user, and will take up his appointment in May 2008. We are looking forward to having Terry back with us again, in what promises to be a very busy year for Gemini with NICI, Flamingos-2, and GSAOI to be commissioned on Gemini South, and GNIRS being recommissioned on Gemini North.

One of the first tasks to be carried out by the new AusGO, even before its formal move to the AAO, was the recruitment of the 2007/08 Australian Gemini Undergraduate Summer Students (AGUSS). Under this scheme, 3 Australian undergraduate students get to spend 10 weeks working at the Gemini South headquarters in La Serena, Chile on a research project supervised by Gemini staff. In addition to visits to the Gemini South telescope, they will also participate in a lecture course offered by CTIO in conjunction with the US-equivalent Research Experience for Undergraduates scheme. The 2007/08 AGUSS recipients are Emily Craven (U. Adelaide), Jacinta Delhaize (U. Western Australia), and Richard Linossi (Monash U.).

The Gemini Observatory publishes its own twice-yearly newsletter, "Gemini Focus" available electronically from http://www.gemini.edu/index.php?option=content&task=view&id=27.

Printed copies are distributed by AusGO to interested Australian readers. If you would like to receive a printed copy, please let us know by e-mailing "ausgo@aao.gov.au". We plan to publish Gemini news and items with a more specific Australian focus here in the AAO Newsletter, as well as on the new AusGO web site at http://ausgo.aao.gov.au .

LETTER FROM COONABARABRAN

Rhonda Martin

Well, it's done, the mammoth job of removing asbestos from Site. The workshop, UKST and the AAT ….. all safe and sound and the AAT sparkles in its new skin. It was a very interesting job to watch, as the old Galbestos was unscrewed, swung out, wrapped and despatched for safe disposal. For safety in high winds two cranes were used, one to lower and one to control, and as the wind caught the sheets and whipped the cranes on their long jibs around it was real heart-in-the-mouth stuff, but these men were experts and even in their heavy cold-weather gear handled it all with aplomb.

Farewelled last year was our Engineer, Allan Lankshear. Allan had been with the AAO for 18 years and opted for a mountain-top barbeque to celebrate his retirement. Being winter it was freezing so while the hardy cooks tended the meat the rest of us made a bee-line for the warmth of the Lodge. It was a very pleasant lunch and Allan much appreciated his gift of David Malin's new book, some framed photographs of the skies and his local gift, made by Mick Kanonczuk

We would like to introduce our two new Night Assist-ants, Yuriy Kondrat from Ukraine and Winston Campbell, previously with the RSAA. Yuriy is a big-city boy from Kiev so Coonabarabran has been a bit of a culture shock. Welcome to you both.

Allan Lankshear cutting his farewell cake. (Rhonda Martin)

The Christmas party was held on the mountain top this year with Santa arriving on a ride-on mower, his sleigh having been laid up for repairs. Santa usually comes after the school kids have arrived on the bus. I must admit they did look a little startled to see him arrive on the mower but they took it in their stride. It is always worth it, just to see their faces.

Castlereagh River near its headwaters. (Martin Oestreich)

This was just a couple of weeks before the most start-tling downpouring of rain. It has been a long time since we have seen so much water – approximately 250 mm in 12 hours – a quantity which left us gasping, had creeks racing for the first time in years, and which then ran into the astonished Castlereagh, grown accustomed to som-nolence over the past few years. In revenge for the onslaught it discharged the water downstream to wreak havoc in Coonamble and other towns in the flat country. The flood peak is making its way toward the Darling River and should give that overstressed system a breath of life.

Opened recently was the Virtual Solar System, a built-to-scale model which uses Siding Spring as the Sun (although we have so far resisted pressure to paint the dome bright yellow). This has caused a great deal of interest with tourists, often seen having their picture taken standing in front of Earth, or Jupiter, or most impres-sively, Saturn. This was the brainchild of John Shobbrook, now of the Faulkes Telescope, and has taken quite a few years to bring to fruition. It gives a very good idea of the immensity of space, and our solar system – Mercury, Venus and Earth are on Siding Spring Mountain, then Mars a few hundred metres along Timor Road, Jupiter several kilometres further on but still on Timor Road. Then there are increasing distances for the remaining planets with Pluto somewhere near Dubbo. It is quite disconcerting to be driving along an empty road when suddenly Saturn looms on the hori-zon, usually with a vulture sitting on it, waiting for tourists!

SUMMER STUDENTS

Paul Dobbie

The AAO runs a twice-yearly student fellowship programme to enable undergraduates to gain first hand experience of astronomical related research. Our current students are from the southern hemisphere. Emily Brunsden has recently completed an honours degree in Astronomy at the University of Canterbury, New Zealand. She is working with Stuart Ryder on a study of the supernova 2001ig. Recent observations of this supernova obtained at radio wavelengths have revealed unusual periodic density fluctuations in the circumstellar medium which may be linked to the presence of a hot stellar companion. To examine this object more closely, new long-slit spectra of SN 2001ig and its surroundings have been obtained with the Gemini South telescope in 2007. Emily is reducing and analysing these data to look for the spectral signature of the surviving companion star.

Silvie Ngo is a third year science and engineering student from the Australian National University and is working with Simon Ellis on a study of the formation of low mass galaxies in clusters at redshift z = 0.5. In the hierarchical model of structure formation, massive galaxies form through mergers of less massive galaxies, so it is expected that the former will contain young stars and that the latter will contain old stars. However, observations reveal that less massive galaxies are young and predominantly blue in colour, hinting that these structures undergo star formation at a later epoch than their more massive cousins. This is a phenomenon known as galaxy downsizing. Silvie is using J, H and K imaging data obtained from the SQIID instrument on the 4m telescope at Kitt Peak National Observatory to search for an environmental dependence of downsizing. It may be possible to reconcile hierarchical merging and galaxy downsizing if the latter is found to be dependent on environment.

Our third student is Andrew Kels from the University of Queensland. He has recently completed a BSc. degree in maths and physics and is working with Matthew Colless and Heath Jones on a study of early-type galaxies and the Fundamental Plane. The Fundamental Plane is a relation linking the mass, size and luminosity of early-type galaxies. These parameters are now available for more than 10,000 bright early-type galaxies as an outcome of the recently completed 6dF Galaxy Survey. Andrew's investigation will address a key question about the formation of early-type galaxies: is the form of the Fundamental Plane purely determined by the physics of galaxy formation on relatively small scales, or is it also affected by the large-scale structures in which galaxies are embedded?

EPPING NEWS

Sandra Ricketts

This issue of the newsletter sees us again farewelling several colleagues. John Dawson left us for the private sector in September, Katrina Tapia-Sealey in December and Katie Powell, our receptionist, left at the end of the year. Goodbyes were said to John and Katie at two enjoyable lunches, and to Katrina at a special morning tea . We wish them all well in their future endeavours and hope that they will continue to keep in touch with us.

One person who does keep in touch, and in fact is seen around Epping frequently, is Scott Croom, and congratulations are due to him and Lindsay on the birth of their third son, Charlie. And Joss Hawthorn is also to be found at Epping on a fairly regular basis.

Congratulations of a different kind are also due to Roger Haynes, who is our new Head of Instrument Science, and to Stuart Ryder, who is the new Australian Gemini Scientist (see page 37 in this issue).

Fred Watson has published another book, "Why is Uranus Upside-down?" and a launch was organised in the conference room in early December. Fred was kept busy signing numerous copies, while the rest of us enjoyed the refreshments amid Christmas decorations. And then we had the AAO Christmas party in Lane Cove National Park. Staff, students and family members all had a great afternoon, with lots of games, contests, carol singing accompanied by Sam Barden on the violin and delicious food.

The AAO citizenship quiz at the AAO Christmas party caused much wracking of brains. (Stuart Ryder)

THE BACK PAGE

Coronal magnetic maps of the components of HD155555

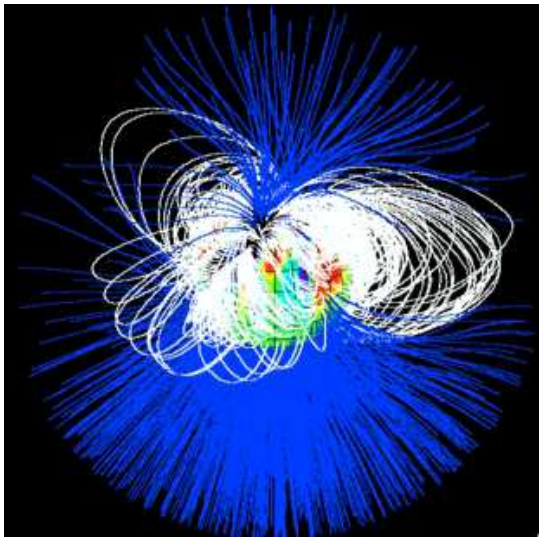

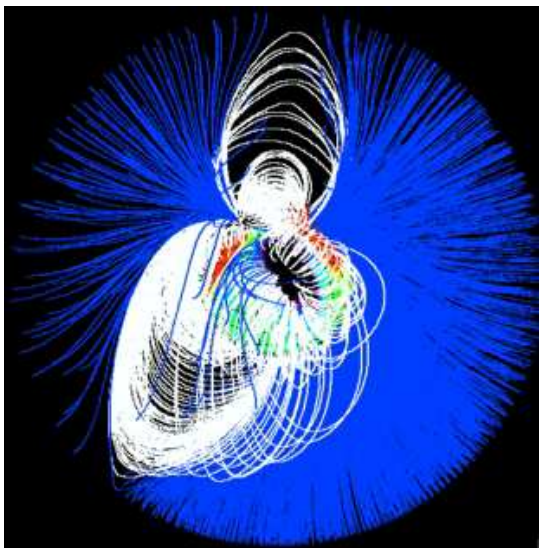

The two figures show coronal magnetic field lines for the primary (top) and secondary (bottom) of the active pre-main sequence binary HD155555, with closed field lines in white and open in blue. The coronal field has been extrapolated from magnetic field topologies of the two stars created from AAT observations. The primary star's magnetic axis has a ~30° misalignment with the rotational axis while for the secondary there is a ~75° difference between the alignment of the two axes. (Moira Jardine, Uni. of St Andrews).

editor PAUL DOBBIE editorial assistant SANDRA RICKETTS

ISSN 0728-5833
Published by ANGLO-AUSTRALIAN OBSERVATORY
PO Box 296 Epping, NSW 1710 Australia

Epping Lab
Telephone +61 2 9372 4800 Fax +61 2 9372 4880 email < *user*@aaoepp.aao.gov.au >

AAT/Schmidt
Telephone +61 2 6842 6291 Fax +61 2 6884 2298 email < *user*@aaocbn.aao.gov.au >

URL < http://www.aao.gov.au >